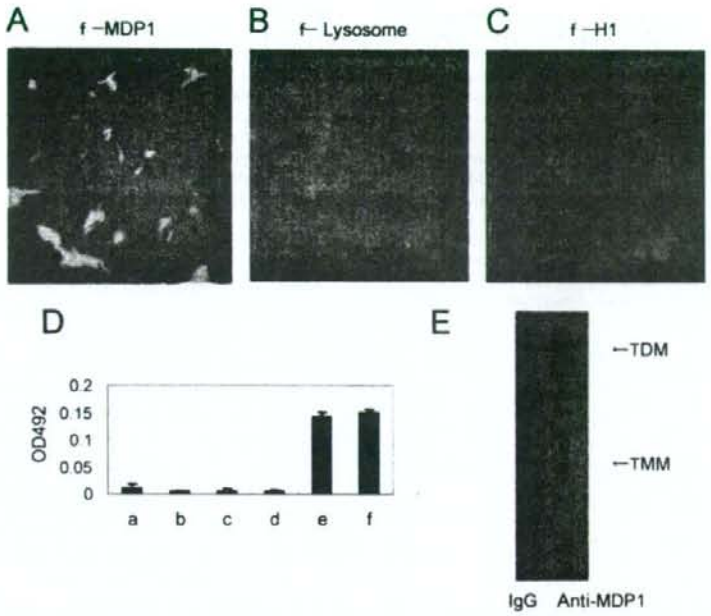

FIG. 1. MDP1 binds to the cell wall of BCG. (A to C) BCG was incubated with FLUOS-labeled MDP1 (A), egg white lysozyme (B), and bovine histone H1 (C). Bacteria were viewed with a confocal scanning laser microscope. (D) ELISA to detect MDP1-lipid or -glycolipid interactions. Mycolic acids (bar b, alpha-MAME; bar c, methoxy-MAME; bar d, keto-MAME) and glycolipids (bar e, TMM; bar f, TDM) were immobilized on an ELISA plate and reacted with MDP1, and the level of binding was detected with anti-MDP1 MAb 3A. Bar a shows the results for a negative control without immobilization of either lipids or glycolipids. OD492, optical density at 492 nm. (E) Immunoprecipitation assay to detect physiological interaction of MDP1 and glycolipid. Cell wall derived from BCG was incubated with anti-MDP1 MAb 3A or control mouse IgG in the presence of protein G-coated Sepharose. Samples were spotted on a TLC plate and developed with the chloroform-methanol-acetone-acetic acid (80:20:6:1, vol/vol/vol/vol) solvent system.

MDP1 regulates transfer of mycolic acids by Ag85 complex proteins in vitro. We next examined the effect of MDP1 on transfer of mycolic acids by Ag85 complex proteins, because MDP1 can bind TMM and TDM, which are substrates of Ag85 complex proteins. We purified Ag85 complex proteins, as well as Ag85A, Ag85B, and Ag85C individually, from *M. tuberculosis* H37Rv by the method described previously (28). Purified Ag85 complex proteins transferred mycolic acids to ^{14}C-labeled trehalose as described previously (4). A molar amount of MDP1 equivalent to that of the Ag85 complex reduced synthesis of TDM and TMM by 44.4% ± 18.4% and 57.4% ± 25.2%, respectively (Fig. 2A and 2B). In contrast, a molar ratio of MDP1 to Ag85 proteins of 1/1,000 enhanced synthesis of TDM and TMM by 36.8% ± 32.4% and 36.4% ± 22.1%, respectively (Fig. 2A and 2B). The same results were obtained when total culture filtrates were used (Fig. 2C, upper chromatogram) or when purified Ag85B was used (Fig. 2C, lower chromatogram). These results demonstrate that MDP1 possesses an activity to control the function of mycolyltransferases.

MDP1 binds to Ag85 complex proteins. Because MDP1 controlled transfer of mycolic acids in the presence of excess amounts of substrate (TMM) (Fig. 2), we considered the possibility that MDP1 interacts not only with TMM but also with Ag85 complex proteins, which we examined next. Ag85A, Ag85B, or Ag85C was immobilized on ELISA plates by serial concentration and then incubated with MDP1. The level of binding of MDP1 to Ag85 complex proteins was detected by anti-MDP1 MAb. The results showed that the interaction between MDP1 and each Ag85 complex protein produced standard binding curves (Fig. 3A). BSA did not bind to MDP1. These results suggested that MDP1 binds to all Ag85 proteins.

Ag85 complex proteins bind to fibronectin by the motif conserved in the complex, which is comprised of 11 amino acid residues (29). We examined if this region also participated in the MDP1-Ag85 complex protein interaction. However, neither human fibronectin nor synthetic peptide corresponding to the region from position 98 to position 108 of Ag85B, which inhibits an Ag85 complex-fibronectin interaction, inhibited an MDP1-Ag85 complex protein interaction (data not shown). Thus, Ag85 complex proteins associate with MDP1 through a region other than the fibronectin-binding site.

We next examined whether MDP1 interacted with Ag85 complex proteins in the mycobacterial cell wall. A cell wall fraction derived from BCG was immunoprecipitated with MAb 3A or control mouse IgG and separated by SDS-PAGE. One gel was stained with Coomassie brilliant blue R250, and another gel was used for Western blot analysis. Although we observed only faint bands corresponding to Ag85 complex proteins (Ag85A and Ag85C at 32 kDa and Ag85B at 30 kDa) in the stained gel, in the Western blot analysis we observed that the bands reacted with anti-Ag85 complex protein Ig in the

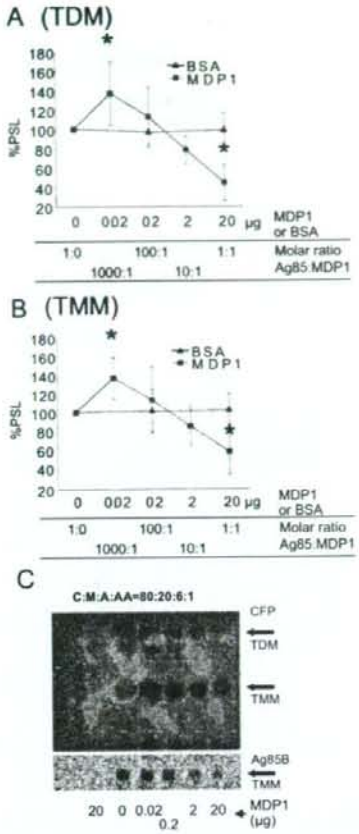

FIG. 2. MDP1 regulates mycolyltransferase activity in vitro. (A and B) Radioactivity of ^{14}C-labeled TDM (A) and TMM (B) synthesized by Ag85 complex proteins in vitro was quantified by using the BAS system software. Radioactivity was expressed as a percentage of the value for the sample without MDP1, which was defined as 100%. Similar experiments were performed utilizing BSA instead of MDP1, and the results were compared. PSL, photo-stimulated luminescence. Asterisk, $P < 0.05$ for a comparison with control BSA (0 or 20 μg) (as determined by analysis of variance). (C) Culture filtrate (CFP) (upper chromatogram) or Ag85B (lower chromatogram) was added to each vial and incubated for 30 min at 37°C in the presence of various doses of MDP1 and [^{14}C]trehalose, and then glycolipids were eluted with chloroform-methanol (2:1, vol/vol). Biosynthesis of glycolipids was analyzed by using the BAS system after TLC plates were developed with the chloroform-methanol-acetone-acetic acid (C:M:A:AA) (80:20:6:1, vol/vol/vol/vol) solvent system. The lane on the left contained a negative control without culture filtrate and Ag85B.

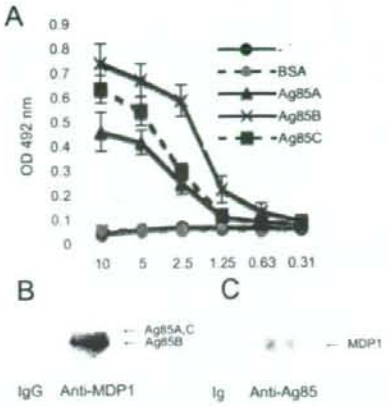

FIG. 3. MDP1 binds to Ag85 complex proteins. (A) ELISA to detect the MDP1-Ag85 complex protein interaction. BSA, Ag85A, Ag85B, and Ag85C were immobilized on an ELISA plate by incubating various concentrations of proteins and reacted with MDP1, and the binding was detected with anti-MDP1 MAb. −, results without immobilized proteins. OD 492 nm, optical density at 492 nm. (B and C) Immunoprecipitation assay to detect a physiological interaction between MDP1 and Ag85 complex proteins. Cell walls derived from BCG were incubated with (B) anti-MDP1 MAb 3A (Anti-MDP1) or control mouse IgG (IgG) or (C) with anti-Ag85 Ig (Anti-Ag85) or control rabbit Ig (Ig) in the presence of protein G-coated Sepharose. Samples for Western blotting were probed with rabbit anti-Ag85 Ig (B) or anti-MDP1 MAb (C).

precipitates when anti-MDP1 MAb was used but not when control IgG was used (Fig. 3B). Similar experiments were performed with anti-Ag85 Ig. Anti-Ag85 Ig, but not control Ig, precipitated MDP1 from the cell wall fraction of BCG (Fig. 3C). Taken together, these results suggest that the Ag85 complex proteins associate with MDP1 in the cell wall.

Subcellular localization of MDP1 in the course of culture. We analyzed the MDP1 content of the cell wall during the course of culture. We cultured *M. smegmatis* in LB medium for 3, 5, and 7 days, and each subcellular fraction was purified. In this experiment, bacteria grew to stationary phase by day 4 (Fig. 4A). The MDP1 content in each fraction was analyzed by Western blotting. The results showed that MDP1 accumulated in both cell wall and other cellular fractions (membrane, ribosome, and cytoplasmic fractions) at the stationary growth phase (Fig. 5A).

We next carried out a similar experiment with BCG. Total cellular proteins, the cell wall fraction, and other cellular fractions were obtained from BCG after growth for 10, 20, 30, and 60 days on Sauton medium. A Western blot analysis showed that the cellular content of MDP1 increased in both the cell wall and other cellular fractions (Fig. 5B), while the levels of Ag85 complex proteins in the cell wall decreased with time (Fig. 5C).

Role of MDP1 in glycolipid biosynthesis. MDP1 is presumed to be essential in slow growers, such as *M. tuberculosis* (34). However, the *mdp1/hlp* gene can be knocked out in *M. smegmatis* (19). In order to determine the physiological role of MDP1 in assembly of the cell wall, we employed an *M. smegmatis* MDP1/HLP KO strain constructed by the group of Thomas Dick (19). We additionally generated an MDP1-complemented strain by insertion of a single copy of the *M. smegmatis* MDP1 gene into the genome of the MDP1/HLP KO strain.

We first analyzed the growth kinetics of the wild type, the MDP1 KO strain, and the complemented strain in LB medium. In this experiment, all strains reached stationary phase on day 4, but the bacterial density of the MDP1 KO strain was lower than that of the wild-type strain during the stationary growth

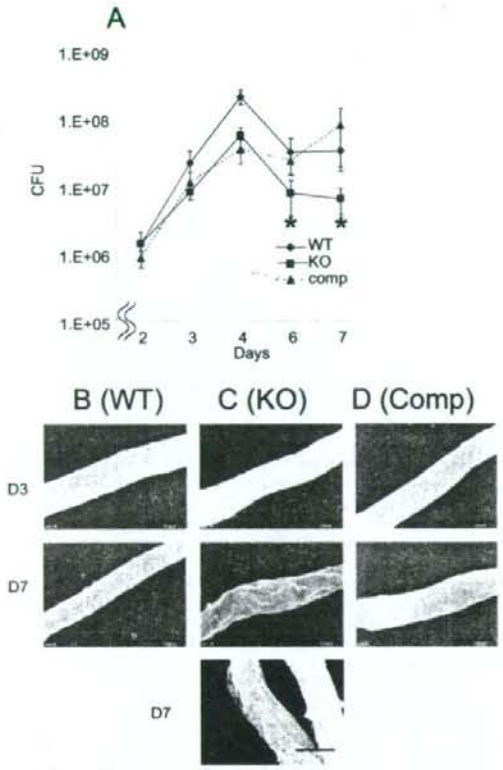

FIG. 4. Effect of MDP1 deficiency on growth kinetics and cell surface morphology. (A) Wild-type *M. smegmatis* mc^{2}155, MDP1 KO, and complemented strains were cultured in LB broth, and bacterial numbers at various time points were determined and expressed as CFU after serially diluted samples on LB agar were harvested. Asterisk, $P < 0.05$ for a comparison with the wild-type strain (as determined by analysis of variance). The results are the results of one representative experiment of seven experiments in which similar results were obtained. (B to D) Visualization of cell surface structure of the wild-type (WT) (B), MDP1 KO (KO) (C), and complemented (Comp) (D) strains by SEM. Bars = 0.5 μm. Bacteria in both exponential (day 3 [D3]) and stationary (day 7 [D7]) phases were analyzed.

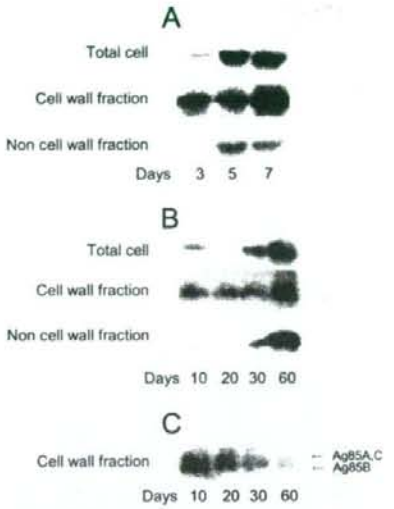

FIG. 5. Subcellular localization of MDP1 and Ag85 in the course of culture. (A to C) Total cellular protein (Total cell), the cell wall fraction (Cell wall fraction), and the residual material after isolation of the cell wall fraction (Non cell wall fraction) were obtained from *M. smegmatis* (A) and BCG (B and C) at each time point indicated. The samples were analyzed by Western blotting with anti-MDP1 MAb 3A (A and B) or anti-Ag85B Ig (C). The data are representative of three to five experiments.

phase (Fig. 4A). This phenotype was almost completely reversed by complementation. Next, we analyzed bacterial surface morphology by SEM. All strains produced similar smooth structures at exponential phase (Fig. 4B, C, and D, upper panels), and both the wild-type and complemented strains were normal with a smooth shape even in the stationary growth phase (Fig. 4B and D, middle panels). However, at the same time point, the MDP1 KO strain displayed a crenellated structure (Fig. 4C, middle and lower panels), implying that MDP1 influences cell envelope structure during stationary phase in *M. smegmatis*.

In order to analyze the effect of MDP1 disruption on glycolipid biosynthesis, we chased synthesis of mycolates and TMM by adding ^{14}C-labeled acetic acid to cultures of the wild-type, MDP1 KO, and complemented strains. Incorporation of radioactivity into TMM and MAMEs was analyzed by using the BAS system after fractionation by high-performance TLC (Fig. 6). TLC analysis revealed two TMM spots (Fig. 6A). *M. smegmatis* produces three types of mycolic acids, alpha, alpha′, and epoxy mycolates. To determine which types of mycolates were present in each TMM spot, we determined the molecular mass of each spot by MALDI-TOF mass spectrometry. The major peak of the upper TMM spot showed a pseudomolecular ion $[M+Na]^+$ at *m/z* 1556, which was identified as alpha-C_{83} TMM, while the major peak of the lower spot showed a pseudomolecular ion $[M+Na]^+$ at *m/z* 1306, which was presumed to be alpha′-C_{65} TMM (data not shown) (14). Thus, high-performance TLC analysis can separate alpha TMM and alpha′ TMM.

The three strains synthesized similar amounts of TMM and MAMEs during exponential growth (day 3). However, during stationary phase (day 7), in both the wild-type and complemented strains mycolate synthesis was reduced strongly (day 7). By contrast, the MDP1-deficent strain continued production of both mycolates and TMM, synthesizing 9.9-fold-higher amounts of TMM (Fig. 6B), 4.3-fold-higher amounts of alpha-MAME (Fig. 6C), and 5.9-fold-higher amounts of alpha′-MAME (Fig. 6D) than the wild type. This phenotype was completely reversed by complementation, indicating that a lack of MDP1 impaired the down-regulation of biosynthesis of mycolates and TMM in stationary phase.

Altering the growth rate with Ag85 complex proteins and MDP1. Because cell wall biogenesis is a biological event involved in multiplication of bacteria, we next examined whether regulation of the transfer of mycolic acids by MDP1 influences mycobacterial growth. We assessed the effects of exogenously

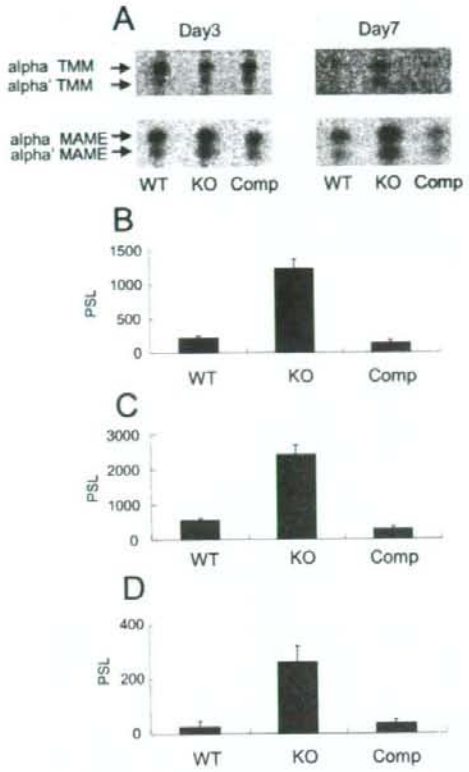

FIG. 6. MDP1 mediates cessation of glycolipid biosynthesis at the stationary growth phase. (A) Lipid synthesis was measured by addition of [^{14}C]acetate to a bacterial culture. The TMM and MAMEs from 10^8 bacteria, including the *M. smegmatis* parent strain (wild type [WT]), the MDP1 KO strain (KO), and the complemented strain (Comp), were extracted on days 3 and 7 and fractionated by TLC. The radioactivities of synthesized TMM and MAMEs were visualized by using the BAS system. (B to D) Radioactivities of TMM (B), alpha-MAME (C), and alpha'-MAME (D) extracted from a bacterial culture after 7 days were quantified by using the BAS system software and compared for the wild-type, MDP1 KO, and complemented strains. The values are means ± standard deviations of five experiments. PSL, photostimulated luminescence.

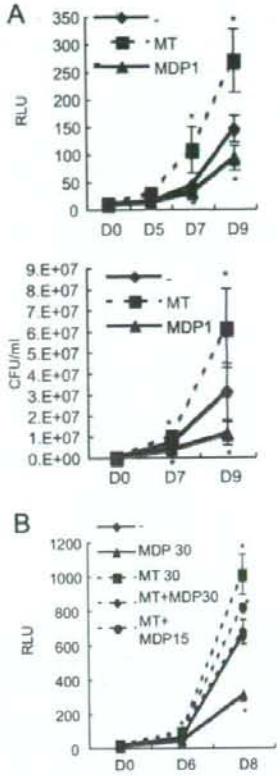

FIG. 7. Growth control of BCG by exogenously added MDP1 and Ag85 complex proteins. BCG-Luc was grown in RPMI 1640 containing 10% FBS in the presence of various doses of MDP1, Ag85 complex, or a mixture of MDP1 and the Ag85 complex in a 96-well tissue culture plate. The total culture volume was 200 μl in each well. Representative results of three independent experiments are presented. (A) Luciferase activity (expressed in relative luciferase units [RLU]) was measured on days 0, 5, 7, and 9 (upper graph), and CFU were counted on days 0, 7, and 9 (lower graph). MT, 30 μg/well Ag85 complex; MDP1, 30 μg/well MDP1; −, BCG-Luc alone. The values are the means ± standard deviations of three experiments. (B) Luciferase activity was measured on days 0, 6, and 8. MT 30, 30 μg/well Ag85 complex; MDP 30, 30 μg/well MDP1; MT + MDP30, 30 μg/well Ag85 complex plus 30 μg/well MDP1; MT + MDP15, 30 μg/well Ag85 complex plus 15 μg/well MDP1; −, BCG-Luc alone. The values are the means ± standard deviations of three experiments. Asterisk, $P < 0.05$ for a comparison with the no-protein control (as determined by analysis of variance).

added MDP1 in culture media on this growth. We generated a luciferase-producing BCG strain (BCG-Luc) to estimate the growth of BCG. The activity of luciferase paralleled the CFU assay results up to 10^4 CFU/ml (data not shown). We cultured BCG-Luc in the presence or absence of MDP1 or Ag85 complex proteins. Both the luciferase-based assay and determination of the CFU showed that exogenously added MDP1 suppressed growth of BCG, while Ag85 complex proteins enhanced growth (Fig. 7A). We next added serial doses of MDP1 to the culture of BCG-Luc in the presence of Ag85 complex proteins. We found that a low dose of MDP1 further boosted Ag85 complex-induced growth enhancement, while a high dose of MDP1 suppressed Ag85-dependent growth enhancement (Fig. 7B).

DISCUSSION

In this study, we analyzed the role of the mycobacterial histone-like protein MDP1 in the cell wall. We found that MDP1 plays an important role in tuning cell wall assembly by controlling transfer of mycolic acids to sugars by Ag85 complex proteins.

We showed that the cellular content of MDP1 was increased in advanced cultures of both *M. smegmatis* and BCG (Fig. 5). Previously, we and other groups showed that MDP1/HLP was accumulated in growth-retarded phases, including dormant bacilli of *M. tuberculosis* and *M. smegmatis* (19, 26, 37), by one-

dimensional SDS-PAGE analysis. MDP1 is resistant to analysis by two-dimensional gel electrophoresis because of its strong positive charge (pI of BCG, 12.4; pI of *M. tuberculosis*, 12.45). However, in spite of the extensive analysis of gene expression profiles with DNA microarrays, increased expression of *mdp1* mRNA in a stationary or anaerobic culture has not been observed (5, 18, 30, 35, 42). These results imply that accumulation of MDP1 in growth-retarded phases is largely due to posttranscriptional regulation. Pethe et al. found that lysines of the C-terminal region of laminin-binding protein/MDP1 are methylated by an unknown enzyme, which is present at a high level in the cell wall and confers resistance to proteolysis (31). Thus, posttranslational modification stabilizes MDP1 and might be involved in accumulation of MDP1 during a growth-retarded phase. In addition, methylation of basic charged amino acids may help the association of MDP1 with glycolipids by negating the charge of the protein. Posttranslational modifications, resembling eukaryotic histones, may control the cellular function and stability of MDP1. This issue should be clarified by additional study. By contrast, Ag85 complex proteins were localized in the cell wall during culture, but the contents gradually decreased with time in BCG (Fig. 5C) and *M. smegmatis* cultures (data not shown). It is likely that mycobacteria regulate transfer of mycolic acids by altering amounts of both MDP1 and Ag85 complex proteins in the cell wall.

The density of the MDP1 KO strain was lower in stationary phase (Fig. 4A). Lee et al. reported that an HLP/MDP1 KO strain displayed the same growth kinetics in Dubos Tween-albumin broth (19). We confirmed that an *M. smegmatis* MDP1 KO strain exhibited similar levels of cell density and survival at stationary phase when it was cultured in Dubos Tween-albumin broth (data not shown). Furthermore, alteration of the surface structure at stationary phase was not revealed by SEM analysis of the surface of the MDP1 KO strain cultured in Dubos Tween-albumin broth (data not shown).

TMM-derived mycolic acids are a major source of TDM and AG-linked mycolic acids (40, 41). Thus, the amount of TMM is an important factor for determining the level of cell wall assembly. The MDP1 KO strain exhibited continued synthesis of TMM other than MAMEs (Fig. 6) and TDM (data not shown) at the stationary growth phase. TMM could be synthesized from TMM and TDM by Ag85 complex proteins, once the substrates (TMM and TDM) were synthesized. However, the primary enzyme that catalyzes synthesis of TMM is still not known. Takayama et al. proposed that TMM could be synthesized in the cytoplasm (40). However, recently, Tropis et al. demonstrated that TMM is synthesized outside the plasma membrane but not inside the cytoplasm (41). The Ag85 complex is the most abundant protein secreted by *M. tuberculosis* (around 10 to 30%) and is a possible candidate enzyme for transfer of mycolic acids to trehalose to synthesize the TMM precursor (β-keto-acyl trehalose), as deduced from the structure of Ag85C (33). MDP1 suppresses Ag85 complex-dependent secondary synthesis of TMM (Fig. 2B), but we cannot eliminate the possibility that MDP1 also inhibits the primary synthesis of the TMM precursor whenever it is catalyzed by Ag85 complex proteins or undetermined enzymes.

An activity controlling glycolipid biosynthesis prompted us to examine whether exogenously added MDP1 and Ag85 complex proteins influence bacterial growth. We showed that growth of BCG could be altered by a combination of Ag85 complex proteins and MDP1 (Fig. 7). The MDP1 content in the total proteins of the cell wall increased at the stationary growth phase, while that of the Ag85 complex proteins decreased (Fig. 3). It can be speculated that a change in the ratio of MDP1 to Ag85 complex proteins in the cell wall is involved in determining the growth rate.

Inhibition of specific cellular metabolism causes cell death, as many antibiotics kill bacteria. However, expression of MDP1 does not kill mycobacteria; instead, it just suppresses growth (23). This is probably due to suppression of whole cellular metabolism, including macromolecular biosynthesis of DNA, RNA, and proteins (23) and cell wall assembly, as shown in this study. This can be caused by multiple interacting activities of different classes of macromolecules. The mechanism of such multiple binding activities should be resolved by structure-based studies, like those done on bacterial proteins such as SecB (32, 44). Recently, it has been reported that the histone-like protein HN-S mediates silencing of global gene expression in growth-retarded *Salmonella* (2, 8, 21). In humans, histone H2A seems to be involved in X chromosome inactivation (11). It can be speculated that use of a nonspecific DNA-binding protein to inactivate cellular metabolism is a general strategy. Here we found an alternative role of a histone-like protein in bacterial metabolism. Our data suggest that MDP1-medaited control of glycolipid biosynthesis is involved in the mechanism linking the growth state and cell wall biogenesis. Although we conducted experiments using nonpathogenic or slightly pathogenic mycobacteria, such as *M. smegmatis* and BCG, these bacteria share the basic structure of the cell wall with pathogenic mycobacteria, including *M. tuberculosis*. Taken together, our data provide significant information for understanding both the coordination of bacterial growth and virulence.

ACKNOWLEDGMENTS

We are grateful to Keizou Oka, Department of Bioscience, INCS, Ehime University, for technical assistance with preparation of MAbs and to Thomas Dick, Novartis Institute for Tropical Diseases, for providing the *M. smegmatis* HLP/MDP1 KO strain. We also thank Todd P. Primm and Charles Scanga for editing the manuscript and Sara Matsumoto for heartfelt encouragement.

This work was supported by grants from the Ministry of Health, Labor and Welfare (Research on Emerging and Re-emerging Infectious Diseases, Health Sciences Research Grants), The Japan Health Sciences Foundation, the Ministry of Education, Culture, Sports, Science and Technology, and The United States-Japan Cooperative Medical Science Program against Tuberculosis and Leprosy.

We have no competing interests.

REFERENCES

1. **Aoki, K., S. Matsumoto, Y. Hirayama, T. Wada, Y. Ozeki, M. Niki, P. Domenech, K. Umemori, S. Yamamoto, A. Mineda, M. Matsumoto, and K. Kobayashi.** 2004. Extracellular mycobacterial DNA-binding protein 1 participates in *Mycobacterium*-lung epithelial cell interaction through hyaluronic acid. J. Biol. Chem. **279:**39798–39806.
2. **Asakura, H., K. Kawamoto, T. Shirahata, and S. Makino.** 2004. Changes in *Salmonella enterica* serovar Oranienburg viability caused by NaCl-induced osmotic stress is related to DNA relaxation by the H-NS protein during host infection. Microb. Pathog. **36:**147–151.
3. **Barry, C. E., III, R. E. Lee, K. Mdluli, A. E. Sampson, B. G. Schroeder, R. A. Slayden, and Y. Yuan.** 1998. Mycolic acids: structure, biosynthesis and physiological functions. Prog. Lipid Res. **37:**143–179.
4. **Belisle, J. T., V. D. Vissa, T. Sievert, K. Takayama, P. J. Brennan, and G. S. Besra.** 1997. Role of the major antigen of *Mycobacterium tuberculosis* in cell wall biogenesis. Science **276:**1420–1422.

5. **Betts, J. C., P. T. Lukey, L. C. Robb, R. A. McAdam, and K. Duncan.** 2002. Evaluation of a nutrient starvation model of *Mycobacterium tuberculosis* persistence by gene and protein expression profiling. Mol. Microbiol. **43:** 717–731.
6. **Bloom, B. R.** 2002. Tuberculosis—the global view. N. Engl. J. Med. **346:** 1434–1435.
7. **Brennan, P. J., and H. Nikaido.** 1995. The envelope of mycobacteria. Annu. Rev. Biochem. **64:**29–63.
8. **Chen, C. C., H. Y. Wu, M. Y. Chou, C. H. Huang, and A. Majumder.** 2005. LeuO protein delimits the transcriptionally active and repressive domains on the bacterial chromosome. J. Biol. Chem. **280:**15111–15421.
9. **Cole, S. T., R. Brosch, J. Parkhill, T. Garnier, C. Churcher, D. Harris, S. V. Gordon, K. Eiglmeier, S. Gas, C. E. Barry III, F. Tekaia, K. Badcock, D. Basham, D. Brown, T. Chillingworth, R. Connor, R. Davies, K. Devlin, T. Feltwell, S. Gentles, N. Hamlin, S. Holroyd, T. Hornsby, K. Jagels, A. Krogh, J. McLean, S. Moule, L. Murphy, K. Oliver, J. Osborne, M. A. Quail, M. A. Rajandream, J. Rogers, S. Rutter, K. Seeger, J. Skelton, R. Squares, S. Squares, J. E. Sulston, K. Taylor, S. Whitehead, and B. G. Barrell.** 1998. Deciphering the biology of *Mycobacterium tuberculosis* from the complete genome sequence. Nature **393:**537–544.
10. **Cole, S. T., K. Eiglmeier, J. Parkhill, K. D. James, N. R. Thomson, P. R. Wheeler, N. Honore, T. Garnier, C. Churcher, D. Harris, K. Mungall, D. Basham, D. Brown, T. Chillingworth, R. Connor, R. M. Davies, K. Devlin, S. Duthoy, T. Feltwell, A. Fraser, N. Hamlin, S. Holroyd, T. Hornsby, K. Jagels, C. Lacroix, J. Maclean, S. Moule, L. Murphy, K. Oliver, M. A. Quail, M. A. Rajandream, K. M. Rutherford, S. Rutter, K. Seeger, S. Simon, M. Simmonds, J. Skelton, R. Squares, S. Squares, K. Stevens, K. Taylor, S. Whitehead, J. R. Woodward, and B. G. Barrell.** 2001. Massive gene decay in the leprosy bacillus. Nature **409:**1007–1011.
11. **Costanzi, C., and J. R. Pehrson.** 1998. Histone macroH2A1 is concentrated in the inactive X chromosome of female mammals. Nature **393:**599–601.
12. **De Voss, J. J., K. Rutter, B. G. Schroeder, H. Su, Y. Zhu, and C. E. Barry III.** 2000. The salicylate-derived mycobactin siderophores of *Mycobacterium tuberculosis* are essential for growth in macrophages. Proc. Natl. Acad. Sci. USA **97:**1252–1257.
13. **Fleischmann, R. D., D. Alland, J. A. Eisen, L. Carpenter, O. White, J. Peterson, R. DeBoy, R. Dodson, M. Gwinn, D. Haft, E. Hickey, J. F. Kolonay, W. C. Nelson, L. A. Umayam, M. Ermolaeva, S. L. Salzberg, A. Delcher, T. Utterback, J. Weidman, H. Khouri, J. Gill, A. Mikula, W. Bishai, W. R. Jacobs, Jr., J. C. Venter, and C. M. Fraser.** 2002. Whole-genome comparison of *Mycobacterium tuberculosis* clinical and laboratory strains. J. Bacteriol. **184:**5479–5490.
14. **Fujita, Y., T. Naka, T. Doi, and I. Yano.** 2005. Direct molecular mass determination of trehalose monomycolate from 11 species of mycobacteria by MALDI-TOF mass spectrometry. Microbiology **151:**1443–1452.
15. **Harlow, E., and D. Lane.** 1988. Antibodies: a laboratory manual. Cold Spring Harbor Laboratory, Cold Spring Harbor, NY.
16. **Jackson, M., C. Raynaud, M. A. Lanelle, C. Guilhot, C. Laurent-Winter, D. Ensergueix, B. Gicquel, and M. Daffe.** 1999. Inactivation of the antigen 85C gene profoundly affects the mycolate content and alters the permeability of the *Mycobacterium tuberculosis* cell envelope. Mol. Microbiol. **31:**1573–1587.
17. **Jacobs, W. R., Jr., M. Tuckman, and B. R. Bloom.** 1987. Introduction of foreign DNA into mycobacteria using a shuttle phasmid. Nature **327:**532–535.
18. **Karakousis, P. C., T. Yoshimatsu, G. Lamichhane, S. C. Woolwine, E. L. Nuermberger, J. Grosset, and W. R. Bishai.** 2004. Dormancy phenotype displayed by extracellular *Mycobacterium tuberculosis* within artificial granulomas in mice. J Exp. Med. **200:**647–657.
19. **Lee, B. H., B. Murugasu-Oei, and T. Dick.** 1998. Upregulation of a histone-like protein in dormant *Mycobacterium smegmatis*. Mol. Gen. Genet. **260:** 475–479.
20. **Liu, J., C. E. Barry III, G. S. Besra, and H. Nikaido.** 1996. Mycolic acid structure determines the fluidity of the mycobacterial cell wall. J. Biol. Chem. **271:**29545–29551.
21. **Lucchini, S., G. Rowley, M. D. Goldberg, D. Hurd, M. Harrison, and J. C. Hinton.** 2006. H-NS mediates the silencing of laterally acquired genes in bacteria. PLoS Pathog. **2:**e81.
22. **Manabe, Y. C., and W. R. Bishai.** 2000. Latent Mycobacterium tuberculosis—persistence, patience, and winning by waiting. Nat. Med. **6:**1327–1329.
23. **Matsumoto, S., M. Furugen, H. Yukitake, and T. Yamada.** 2000. The gene encoding mycobacterial DNA-binding protein 1 (MDP1) transformed rapidly growing bacteria to slowly growing bacteria. FEMS Microbiol. Lett. **182:**297–301.
24. **Matsumoto, S., M. Matsumoto, K. Umemori, Y. Ozeki, M. Furugen, T. Tatsuo, Y. Hirayama, S. Yamamoto, T. Yamada, and K. Kobayashi.** 2005. DNA augments antigenicity of mycobacterial DNA-binding protein 1 and confers protection against *Mycobacterium tuberculosis* infection in mice. J. Immunol. **175:**441–449.
25. **Matsumoto, S., M. Tamaki, H. Yukitake, T. Matsuo, M. Naito, H. Teraoka, and T. Yamada.** 1996. A stable *Escherichia coli*-mycobacteria shuttle vector 'pSO246' in *Mycobacterium bovis* BCG. FEMS Microbiol. Lett. **135:**237–243.
26. **Matsumoto, S., H. Yukitake, M. Furugen, T. Matsuo, T. Mineta, and T. Yamada.** 1999. Identification of a novel DNA-binding protein from *Mycobacterium bovis* bacillus Calmette-Guerin. Microbiol. Immunol. **43:**1027–1036.
27. **Mikusova, K., M. Mikus, G. S. Besra, I. Hancock, and P. J. Brennan.** 1996. Biosynthesis of the linkage region of the mycobacterial cell wall. J. Biol. Chem. **271:**7820–7828.
28. **Naito, M., N. Ohara, S. Matsumoto, and T. Yamada.** 1998. Immunological characterization of alpha antigen of *Mycobacterium kansasii*: B-cell epitope mapping. Scand. J. Immunol. **48:**73–78.
29. **Naito, M., N. Ohara, S. Matsumoto, and T. Yamada.** 1998. The novel fibronectin-binding motif and key residues of mycobacteria. J. Biol. Chem. **273:**2905–2909.
30. **Park, H. D., K. M. Guinn, M. I. Harrell, R. Liao, M. I. Voskuil, M. Tompa, G. K. Schoolnik, and D. R. Sherman.** 2003. Rv3133c/dosR is a transcription factor that mediates the hypoxic response of *Mycobacterium tuberculosis*. Mol. Microbiol. **48:**833–843.
31. **Pethe, K., P. Bifani, H. Drobecq, C. Sergheraert, A. S. Debrie, C. Locht, and F. D. Menozzi.** 2002. Mycobacterial heparin-binding hemagglutinin and laminin-binding protein share antigenic methyllysines that confer resistance to proteolysis. Proc. Natl. Acad. Sci. USA **99:**10759–10764.
32. **Randall, L. L., and S. J. Hardy.** 1995. High selectivity with low specificity: how SecB has solved the paradox of chaperone binding. Trends Biochem. Sci. **20:**65–69.
33. **Ronning, D. R., T. Klabunde, G. S. Besra, V. D. Vissa, J. T. Belisle, and J. C. Sacchettini.** 2000. Crystal structure of the secreted form of antigen 85C reveals potential targets for mycobacterial drugs and vaccines. Nat. Struct. Biol. **7:**141–146.
34. **Sassetti, C. M., D. H. Boyd, and E. J. Rubin.** 2003. Genes required for mycobacterial growth defined by high density mutagenesis. Mol. Microbiol. **48:**77–84.
35. **Schnappinger, D., S. Ehrt, M. I. Voskuil, Y. Liu, J. A. Mangan, I. M. Monahan, G. Dolganov, B. Efron, P. D. Butcher, C. Nathan, and G. K. Schoolnik.** 2003. Transcriptional adaptation of *Mycobacterium tuberculosis* within macrophages: insights into the phagosomal environment. J. Exp. Med. **198:**693–704.
36. **Shimoji, Y., V. Ng, K. Matsumura, V. A. Fischetti, and A. Rambukkana.** 1999. A 21-kDa surface protein of *Mycobacterium leprae* binds peripheral nerve laminin-2 and mediates Schwann cell invasion. Proc. Natl. Acad. Sci. USA **96:**9857–9862.
37. **Shires, K., and L. Steyn.** 2001. The cold-shock stress response in *Mycobacterium smegmatis* induces the expression of a histone-like protein. Mol. Microbiol. **39:**994–1009.
38. **Soares de Lima, C., L. Zulianello, M. A. Marques, H. Kim, M. I. Portugal, S. L. Antunes, F. D. Menozzi, T. H. Ottenhoff, P. J. Brennan, and M. C. Pessolani.** 2005. Mapping the laminin-binding and adhesive domain of the cell surface-associated Hlp/LBP protein from *Mycobacterium leprae*. Microbes Infect. **7:**1097–1109.
39. **Stover, C. K., V. F. de la Cruz, T. R. Fuerst, J. E. Burlein, L. A. Benson, L. T. Bennett, G. P. Bansal, J. F. Young, M. H. Lee, G. F. Hatfull, et al.** 1991. New use of BCG for recombinant vaccines. Nature **351:**456–460.
40. **Takayama, K., C. Wang, and G. S. Besra.** 2005. Pathway to synthesis and processing of mycolic acids in *Mycobacterium tuberculosis*. Clin. Microbiol. Rev. **18:**81–101.
41. **Tropis, M., X. Meniche, A. Wolf, H. Gebhardt, S. Strelkov, M. Chami, D. Schomburg, R. Kramer, S. Morbach, and M. Daffe.** 2005. The crucial role of trehalose and structurally related oligosaccharides in the biosynthesis and transfer of mycolic acids in Corynebacterineae. J. Biol. Chem. **280:**26573–26585.
42. **Voskuil, M. I., D. Schnappinger, K. C. Visconti, M. I. Harrell, G. M. Dolganov, D. R. Sherman, and G. K. Schoolnik.** 2003. Inhibition of respiration by nitric oxide induces a *Mycobacterium tuberculosis* dormancy program. J. Exp. Med. **198:**705–713.
43. **Wayne, L. G., and C. D. Sohaskey.** 2001. Nonreplicating persistence of *Mycobacterium tuberculosis*. Annu. Rev. Microbiol. **55:**139–163.
44. **Zhou, J., and Z. Xu.** 2005. The structural view of bacterial translocation-specific chaperone SecB: implications for function. Mol. Microbiol. **58:**349–357.

Deletion of *kasB* in *Mycobacterium tuberculosis* causes loss of acid-fastness and subclinical latent tuberculosis in immunocompetent mice

Apoorva Bhatt*†‡, Nagatoshi Fujiwara§, Kiranmai Bhatt†¶, Sudagar S. Gurcha‖, Laurent Kremer**, Bing Chen*†, John Chan†, Steven A. Porcelli†, Kazuo Kobayashi§, Gurdyal S. Besra‖, and William R. Jacobs, Jr.*†,††

*Howard Hughes Medical Institute and †Department of Microbiology and Immunology, Albert Einstein College of Medicine, Bronx, NY 10461; §Department of Host Defense, Osaka City University Graduate School of Medicine, Osaka 545-8585, Japan; ‖School of Biosciences, University of Birmingham, Edgbaston, Birmingham B15 2TT, United Kingdom; and **Laboratoire de Dynamique Moléculaire des Interactions Membranaires, Centre National de la Recherche Scientifique, Unité Mixte de Recherche 5539, Université de Montpellier II, 34095 Montpellier Cedex 5, France

Edited by Barry R. Bloom, Harvard School of Public Health, Boston, MA, and approved February 1, 2007 (received for review October 2, 2006)

***Mycobacterium tuberculosis*, the causative agent of tuberculosis, has two distinguishing characteristics: its ability to stain acid-fast and its ability to cause long-term latent infections in humans. Although this distinctive staining characteristic has often been attributed to its lipid-rich cell wall, the specific dye-retaining components were not known. Here we report that targeted deletion of *kasB*, one of two *M. tuberculosis* genes encoding distinct β-ketoacyl- acyl carrier protein synthases involved in mycolic acid synthesis, results in loss of acid-fast staining. Biochemical and structural analyses revealed that the Δ*kasB* mutant strain synthesized mycolates with shorter chain lengths. An additional and unexpected outcome of *kasB* deletion was the loss of ketomycolic acid *trans*-cyclopropanation and a drastic reduction in methoxymycolic acid *trans*-cyclopropanation, activities usually associated with the *trans*-cyclopropane synthase CmaA2. Although deletion of *kasB* also markedly altered the colony morphology and abolished classic serpentine growth (cording), the most profound effect of *kasB* deletion was the ability of the mutant strain to persist in infected immunocompetent mice for up to 600 days without causing disease or mortality. This long-term persistence of Δ*kasB* represents a model for studying latent *M. tuberculosis* infections and suggests that this attenuated strain may represent a valuable vaccine candidate against tuberculosis.**

mycolic acid | Ziehl-Neelsen stain | cording | persistence | FAS-II

The Ziehl–Neelsen stain-based microscopic detection of *Mycobacterium tuberculosis*, which relies on the acid-fast attribute of the tubercle bacillus, remains the cornerstone of diagnosis of tuberculosis (TB), particularly in poor countries where the infection is highly prevalent (1). This staining method was developed by Ziehl and Neelsen who improvised on the early work of Koch, Rindfleisch, and Ehrlich (2–4). Acid-fastness has been attributed to a number of mycobacterial cell wall components, including outer lipids, arabinogalactan-bound mycolic acids (MAs), and free hydroxyl and carboxylate groups of cell wall lipids (5–7). The underlying theme in all of the proposed mechanisms was the presence of a lipid-rich, hydrophobic barrier that could be penetrated by phenol-based stains but was resistant to decolorization by acid-alcohol. However, the precise molecular component responsible for this unique staining property has never been identified.

Early studies on the effects of isoniazid on the staining characteristics of tubercle bacilli demonstrated a loss of acid-fastness after growth in the presence of the antibiotic (8). Because isoniazid was known to inhibit the synthesis of MAs, the major class of lipids composing the cell wall of mycobacteria, this result suggested that these molecules may be the components responsible for the acid-fast staining characteristic and that mutants defective in MA biosynthesis would be reasonable candidates to study the phenomenon of acid-fastness. MAs are very-long-chain α-alkyl β-hydroxy fatty acids that are either esterified to peptidoglycan-linked arabinogalactan or present as a part of the interspersed glycolipid, trehalose dimycolate (TDM) (9, 10). The long mero-MA chain is synthesized by a multienzyme fatty acid synthase II complex (FASII) from acyl carrier protein (ACP)-bound substrates that are elongated by repetitive reductive cycles, the first step of which is catalyzed by a β-ketoacyl-ACP synthase. In *M. tuberculosis* and other mycobacteria, two genes, *kasA* and *kasB*, encode distinct FASII β-ketoacyl-ACP synthases (11). Whereas *kasA* is an essential gene (12), *kasB* is not essential for normal mycobacterial growth in *Mycobacterium marinum* and *Mycobacterium smegmatis* (12, 13), suggesting that *kasB* might be an accessory gene that is not essential for MA biosynthesis. Previous *in vitro* (14) and *in vivo* (13) results had indicated that whereas KasA is involved in the initial elongation of the mero chain, KasB might be responsible for its extension to full-length mero-MAs.

Before this work, the effects of *kasB* deletion in *M. tuberculosis* were unknown, and the role of KasB in pathogenesis had not been investigated in an animal model of infection. In this work, we have shown that the deletion of *kasB* caused alterations in MAs that resulted in a loss of acid-fastness. Furthermore, the *M. tuberculosis* Δ*kasB* mutant was analyzed after infections of both immunocompromised and immunocompetent mice, which revealed a marked attenuation of *in vivo* growth in the mutant that led to a long-term persistent infection that resembled latent tuberculosis. These results provide insights into the nature of the clinically important feature of acid-fast staining in *M. tuberculosis* and are also relevant to understanding and modeling latent tuberculosis.

Results

Deletion of *kasB* Caused a Change in Mycobacterial Colony Morphology and Loss of Cording and Acid-Fastness. A specialized transducing phage, ph*ΔkasB*, containing an allelic exchange substrate designed to replace *kasB* with a hygromycin resistance cassette

Author contributions: A.B., J.C., S.A.P., G.S.B., and W.R.J. designed research; A.B., N.F., K.B., S.S.G., L.K., and B.C. performed research; K.K. and W.R.J. contributed new reagents/analytic tools; A.B., N.F., and K.B. analyzed data; and A.B. and W.R.J. wrote the paper.

The authors declare no conflict of interest.

This article is a PNAS direct submission.

Abbreviations: ACP, acyl carrier protein; FASII, fatty acid synthase II complex; MA, mycolic acid; MAME, mycolic acid methyl ester; TB, tuberculosis; TDM, trehalose dimycolate.

‡Present address: School of Biosciences, University of Birmingham, Edgbaston, Birmingham B15 2TT, United Kingdom.

¶Present address: School of Medicine, St. George's University, Grenada, West Indies.

††To whom correspondence should be addressed. E-mail: jacobsw@hhmi.org.

This article contains supporting information online at www.pnas.org/cgi/content/full/0608654104/DC1.

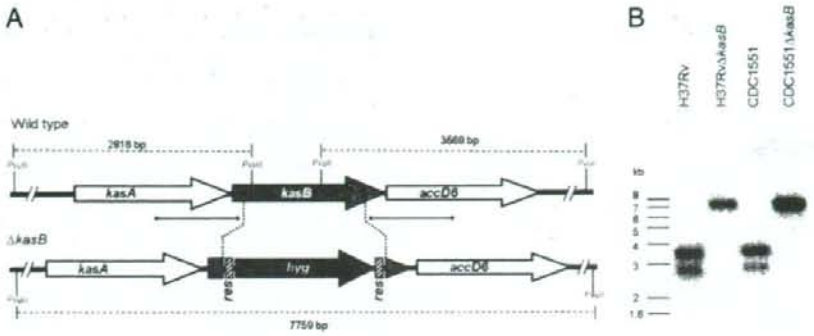

Fig. 1. Generation of a *M. tuberculosis kasB* mutant. (*A*) Map of the *M. tuberculosis kasB* region in WT and Δ*kasB* strains. [α-^{32}P]dCTP-labeled probes were derived from ≈500-bp upstream and downstream flanking sequences that were used to construct the knockout plasmids, and they are indicated by thick lines with square ends. The *PvuII*-digested fragments expected in a Southern blot are indicated by gapped lines with sizes. (*B*) Southern blot of *PvuII*-digested genomic DNA from WT and Δ*kasB* strains. Only one representative band pattern is shown for each mutant strain of H37Rv and CDC1551; *res*, γδ-resolvase site; *hyg*, hygromycin resistance gene.

(*hyg*), was transduced into two virulent *M. tuberculosis* strains, H37Rv (laboratory strain) and CDC1551 (clinical isolate). Southern blot analysis of genomic DNA isolated from hygromycin-resistant (Hyg^R) colonies confirmed replacement of *kasB* with *hyg* (Fig. 1). For further studies, we chose the *kasB* mutant generated in the clinical strain CDC1551; the CDC1551 parental strain, the Δ*kasB* mutant strain, and the complemented strain will be referred to here as WT (wild-type), Δ*kasB*, and Δ*kasB*(pMV261*kasB*), respectively. Deletion of *kasB* resulted in a striking alteration in colony morphology, with the mutant strain forming colonies much smaller than those of the parental strain (Fig. 2). In addition, colonies of mutant strain appeared to have a different surface texture. The smaller size of the colonies was not the result of a slower growth rate because the CDC1551 Δ*kasB* mutant had a doubling rate similar to that of its parental strain when cultured in 7H9 broth (data not shown). WT colony morphology could be restored in the Δ*kasB* mutant upon introduction of *kasB* on a multicopy-replicating plasmid (Fig. 2), indicating that the observed change was due solely to the loss of KasB and not because of a polar effect on the expression of *accD6* located downstream from *kasB*. On the other hand, no complementation was observed with a *kasA*-containing plasmid, indicating that extra copies of *kasA* could not compensate for the loss of *kasB* (data not shown).

A change in colony morphology suggested an altered cell envelope in the Δ*kasB* mutant, and a microscopic examination of cultures grown in 7H9 broth showed that the Δ*kasB* mutant was defective in cording, a classical serpentine growth (Fig. 3). A change in the cell wall composition was further confirmed by acid-fast staining of cultures by two different methods (Kinyoun stain or TB-fluorescent stain), which revealed that the Δ*kasB* strain had lost the ability to retain the primary stain after washing with the acid-alcohol decolorizer (one staining method is shown in Fig. 3). These results suggested that the change in morphology was likely due to a change in the cell wall MA content and correlated well with the increased sensitivity of the Δ*kasB* strain to the lipophilic antibiotic rifampicin (data not shown). The mutant strain was also more sensitive to the KasA/KasB inhibitor thiolactomycin [minimum inhibitory concentration (MIC) <1 μg/ml] than the WT strain (MIC = 5 μg/ml).

MA Chain Length and Cyclopropanation Are Altered in the Δ*kasB* Mutant. The changes in cording and in the acid-fast staining property of the Δ*kasB* strain prompted us to investigate the MA composition of the mutant strain. *M. tuberculosis* produces three classes of MAs: α-, keto-, and methoxy-MAs, each differing in modifications of the mero chain that are catalyzed by distinct cyclopropane synthases, isomerases, and methyl transferases

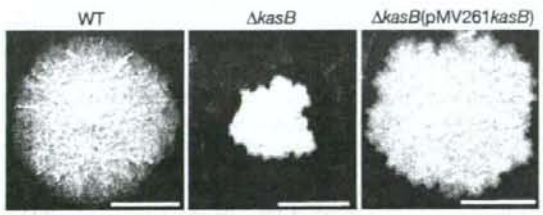

Fig. 2. Colonies of *M. tuberculosis* CDC1551 parental (WT), *kasB* null mutant (Δ*kasB*), and complemented *kasB* mutant [Δ*kasB*(pMV261*kasB*)] strains on 7H10 plates after incubation at 37°C for 4 weeks. (Scale bar, 2 mm.)

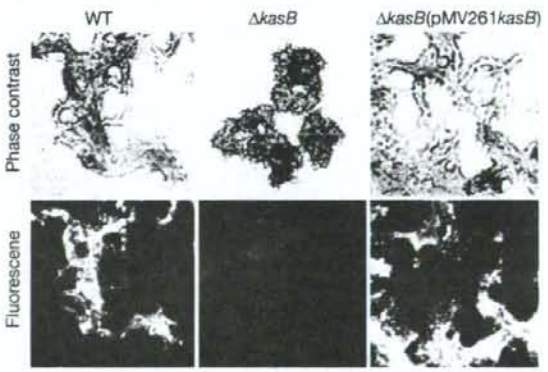

Fig. 3. Light microscopy of *M. tuberculosis* cultures grow static in 7H9 broth at 37°C for 7 days. Cultures were fixed on glass slides, and acid-fast staining was performed on the fixed smears by using the BD TB fluorescent kit-T. (*Upper*) Phase-contrast microscopy images of *M. tuberculosis* WT, Δ*kasB*, and Δ*kasB*(pMV261*kasB*) strains stained with TB-auramine-rhodamine and then treated with acid-alcohol decolorizer. (*Lower*) Fluorescent micrographs of the same fields. (Magnification, ×400.)

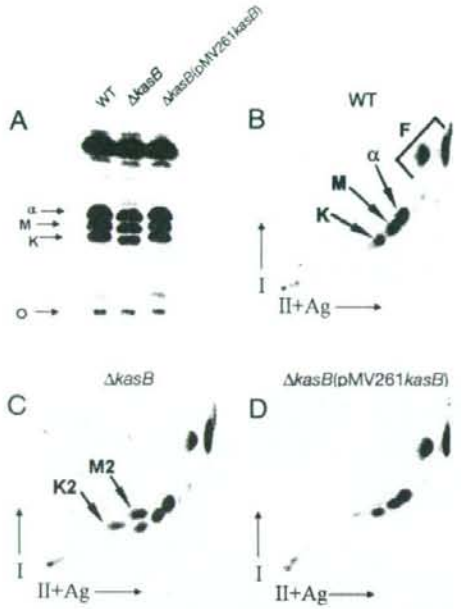

Fig. 4. TLC of ^{14}C-labeled MAMEs from *M. tuberculosis* WT, Δ*kasB*, and Δ*kasB*(pMV261*kasB*) strains. (*A*) Single-dimension HPTLC of MAMEs. (*B–D*) Two-dimensional argentation TLC of WT, Δ*kasB*, and Δ*kasB*(pMV261*kasB*), respectively. O, origin; I, first dimension; II+Ag, second dimension impregnated with $AgNO_3$; α, α-MAMEs; M, methoxy-MAMEs; K, keto-MAMEs; F, fatty acid methyl esters. The two unknown species in the Δ*kasB* strain, M2 and K2, are indicated by arrows.

(15–22). A preliminary analysis of [^{14}C]acetate-labeled MA methyl esters (MAMEs) obtained from total MAs by TLC showed that methoxy- and keto-MAMEs obtained from Δ*kasB* migrated at a slightly lower but reproducible R_f value than those from WT or complemented strains (Fig. 4*A*), suggesting a change in the MA chain lengths. Also, there were differences between the WT and mutant strain with regard to the relative abundance of the three classes of MAMEs: the relative percentages for α-, methoxy-, and keto-MAMEs in total MAMEs from WT strain were 41.5%, 33.5%, and 25%, respectively, and those for the mutant strain were 52%, 32%, and 16%, indicating a decrease in the amount of keto-MAs in the *kasB* mutant [supporting information (SI) Fig. 7]. These defects in MA composition, and the migration in TLCs, were corrected on complementation of Δ*kasB* (Fig. 4*A* and SI Fig. 7). These changes in R_f values and relative abundances of MAs were similar to those observed earlier in a *M. marinum* transposon-disrupted *kasB* mutant (13). Further analysis of MAMEs by two-dimensional argentation TLC (23) (Fig. 4 *B–D*) revealed accumulation of two spots in Δ*kasB* that migrated slightly more slowly than keto- and methoxy-MAME spots in the second dimension (M2 and K2, shown by arrows in Fig. 4*C*). The retarded migration in the second, silver-impregnated, dimension suggested that these spots corresponded to unsaturated MAME species. Similar results were obtained when MAMEs obtained from cell wall-bound MAs and extractable MAs were analyzed separately by two-dimensional TLC, indicating that the altered MAs were esterified to both arabinogalactan and to trehalose (data not shown). No changes in the profiles of other lipids (polar and apolar) were detectable on TLC plates (SI Fig. 8), indicating that the observed phenotypes of Δ*kasB* were likely due to the effects of altered MAs.

Individual MA species were purified from WT, Δ*kasB*, and Δ*kasB*(pMV261*kasB*) and analyzed by MALDI-TOF MS. Spectroscopic data revealed shortened MAs in Δ*kasB* (SI Table 1). The longest α-, methoxy-, and keto-MA species detected in the WT strain were $C_{84:2}$, $C_{92:1}$, and $C_{89:1}$, respectively, whereas in the Δ*kasB* strain the corresponding longest species were $C_{80:2}$, $C_{86:1}$, and $C_{82:1}$, respectively (SI Table 1). In addition, the chain lengths of the most abundant MA species were different in the mutant strain (SI Table 1). Detection of the α-branch by pyrolysis GC revealed that the shortening of chain length was not in the α-branch, but in the mero-MA moiety (SI Fig. 9).

The two accumulated species that were detected by two-dimensional TLC in the Δ*kasB* strain were each found to have a mass identical to the corresponding oxygenated MAME (SI Fig. 10). A more detailed study of purified MAs by ^{1}H NMR analysis revealed the presence of normal levels of *cis*-cyclopropanated methoxy-MAs but diminished resonances for *trans*-cyclopropanated methoxy-MAs in Δ*kasB* (SI Fig. 11). Additionally, no signals corresponding to *trans*-cyclopropanated keto-MAs were detected in the mutant strain (SI Fig. 11).

Furthermore, ^{1}H NMR analysis of total MAs from Δ*kasB* revealed that the two accumulated species in Δ*kasB* were unsaturated precursors of *trans*-cyclopropanated species: signals for *trans*-double bond were detected at 5.24 ppm (J 14.7 Hz) and at 5.34 ppm (J 14.7 Hz) (24), and the protons for the methylene and the methine groups adjacent to the *trans*-double bond were assigned at 1.96 ppm and 2.01 ppm (15, 25) (SI Fig. 12). The protons of the allylic methyl branch of the proximal *trans*-double bond resonated as a doublet at 0.94 ppm (J 6.6 Hz) and the terminal methyl at 0.84 ppm (26, 27). In contrast, spectra of total MAs from the WT strain revealed the absence of allylic methyl branch protons (0.94 ppm) and of *trans*-double bond (5.24 ppm) (data not shown). These results demonstrated that a *trans*-unsaturated precursor of both methoxy- and keto-MAs accumulated in the Δ*kasB* strain.

Loss of KasB in *M. tuberculosis* Causes a Severe Growth *in Vivo* Defect in Mice and Latent Subclinical TB. To assess the effects of altered MAs in the Δ*kasB* strain on mycobacterial virulence, we first tested the ability of the Δ*kasB* mutant to survive in murine (C57BL/6 bone marrow-derived and J774) macrophages and THP-1 cells and found no differences between WT and Δ*kasB* (data not shown). Next, immunocompetent C57BL/6 mice were infected with aerosols of WT, Δ*kasB*, and complemented strains (≈100 bacteria per mouse). Extensive granulomatous inflammation was visible in the lungs of mice infected with the WT or Δ*kasB*(pMV261*kasB*) strains but not in those infected with the Δ*kasB* strain (Fig. 5*A*). Histological examination of stained lung sections from mice infected with the WT or Δ*kasB*(pMV261*kasB*) strains revealed multifocal, moderate infiltration after 21 days of infection (Fig. 5*B*). The severity of the granulomatous lesions increased after 56 days, and after 112 days there was coalescence of lesions into large areas that involved entire lobes of the lung. In contrast, the lungs of mice infected with Δ*kasB* showed more diffuse and less organized infiltrates at 21 days, which decreased in severity after 56 days, and no signs of infection were seen after 112 days (Fig. 5*B*). Consistent with the loss of acid-fastness observed for broth cultures, the *kasB* mutant also failed to retain the primary stain in tissue sections after acid-fast staining and instead took up the methylene blue counterstain (SI Fig. 13).

Monitoring of colony-forming units (cfu) in the lung, spleen, and liver at different time points after infection indicated that the Δ*kasB* mutant was severely attenuated for growth in mice. WT bacteria could replicate extensively in the lung in the first 21 days after aerosol infection, with a three log increase in WT bacteria in infected lungs at the end of 21 days (Fig. 6*A*). In contrast, replication of the Δ*kasB* strain was restricted: bacterial loads in the lung barely increased by 2 orders of magnitude after 21 days of infection and then decreased to between 500 and 1,000

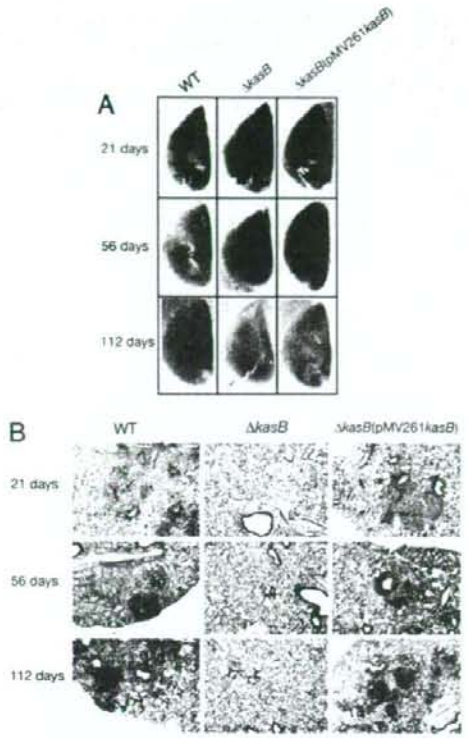

Fig. 5. Pathology of infected mouse lungs. (*A*) Lungs of C57BL/6 mice infected with *M. tuberculosis* WT, Δ*kasB*, and Δ*kasB*(pMV261*kasB*) strains, removed at different time points after aerosol infection. (*B*) Hematoxylin/eosin-stained lung tissue sections from mice infected with WT, Δ*kasB*, or Δ*kasB*(pMV261*kasB*). (Scale bar, 200 μm.)

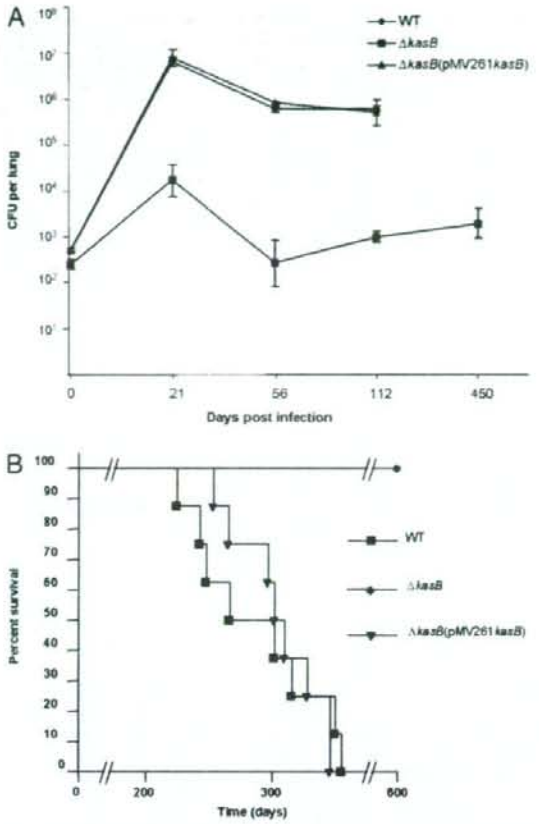

Fig. 6. Attenuation of Δ*kasB* in C57BL/6 mice. (*A*) Plot of *M. tuberculosis* cfu levels in lungs of C57BL/6 mice at different time points after aerosol infection. (*B*) Survival curve of C57BL/6 mice infected with WT, Δ*kasB*, or Δ*kasB* (pMV261*kasB*).

cfu in subsequent weeks (Fig. 6*A*). The Δ*kasB* mutant was also attenuated for growth in liver and spleen (SI Fig. 14 *A* and *B*). Surprisingly, 450 days after aerosol infection, ≈1,000 cfu could still be detected in the lungs of Δ*kasB*-infected mice (Fig. 6*A*), although the mice looked healthy before being killed, which indicated that the mutant was able to persist in the mouse without causing visible signs of disease. Indeed, we observed a significant difference in the mortality of C57BL/6 mice infected by aerosols of the CDC1551 strains (100 cfu per mouse). By day 356, 100% (eight of eight) of the mice infected with WT or Δ*kasB*(pMV261*kasB*) had died (Fig. 6*B*). In stark contrast, all mice infected with Δ*kasB* (eight of eight) were not only alive but also appeared healthy even after 600 days after infection, indicating that Δ*kasB* had failed to cause active infection in the mice. Surprisingly, unlike the results obtained with C57BL/6 mice, the Δ*kasB* strain caused mortality in immunodeficient SCID mice (SI Fig. 15).

Discussion

Our studies demonstrate that the FASII β-ketoacyl-ACP synthase KasB is essential for full MA chain length in *M. tuberculosis*. Although the results of *in vitro* assays suggested that KasB may be involved in elongating a major portion of the mero-MA chain (14), deletion of *kasB* resulted in the shortening of the mero-MA chains by only 2–6 carbons. In addition, the Δ*kasB* mutant lost the ability to synthesize any *trans*-cyclopropanated keto-MAs and produced a miniscule amount of *trans*-cyclopropanated methoxy-MAs, accumulating instead their corresponding unsaturated precursors with *trans*-double bonds, which are putative substrates of the *trans*-cyclopropane synthase CmaA2 (18). This unexpected consequence of *kasB* deletion meant that either the shortened oxygenated mero-MAs are poor substrates for CmaA2 or that CmaA2 interacts preferentially with KasB present in specialized FASIIs, as recently suggested (28, 29). Thus, the deletion of *kasB* had a "downstream phenotypic" effect on *trans*-cyclopropanation of oxygenated MAs, an activity not directly associated with KasB function. In addition, the proportions of the different MA species were also altered, with a reduction in the levels of keto-MAs. These alterations in structure (shortening of MA chain length and loss or reduction of *trans*-cyclopropanation) and in content (reduction in keto-MAs) were observed for both wall-bound and trehalose-bound MAs (data not shown).

Our findings have similarities but also several differences compared with those reported for a transposon-disrupted *kasB* mutant of *M. marinum* (13). In that study, MA species 4 carbons shorter were found compared with up to 6 carbons shorter in the *M. tuberculosis* mutant. We also observed that the deletion of *kasB* affected MA *trans*-cyclopropanation, an activity not detected in WT *M. marinum*. And finally, unlike the *M. marinum* mutant study, we were able to test the ability of the *M. tuberculosis* Δ*kasB* mutant to cause infection in an animal model of infection and thus assess the role of KasB in virulence.

A remarkable change in Δ*kasB* was the complete loss of the acid-fast staining property that is one of the primary defining characteristics of *M. tuberculosis*. Loss of acid-fastness by Δ*kasB* was not only observed in broth cultures but also in infected murine lung tissue. Here again, direct or indirect effects of changes in the MAs of the *kasB* mutant, like a decrease in lipophilicity, may have rendered the cell wall more prone to decolorization with acid-alcohol. It is unlikely that any specific chemical interactions of MAs with the primary stain that were lost in Δ*kasB* could have been responsible for the loss of acid-fastness because two different staining methods (using chemically distinct primary stains) yielded the same results. This work reports the loss of acid-fastness in a specific *M. tuberculosis* mutant that is defective in normal MA biosynthesis, and the only other well characterized acid-fast negative *M. tuberculosis* mutant described has a deletion in *phoP*, which leads to deficiencies of many lipids, including sulfatides, diacyltrehaloses, and polyacyltrehaloses (30). It is worth noting that the deletion of *cmaA2* in *M. tuberculosis* did not alter colony morphology, cording, or acid-fastness (18), indicating that loss of or reduction in *trans*-cyclopropanation can be ruled out as a potential cause of the observed phenotypes in Δ*kasB*.

TDMs are believed to play a particularly important role in determining colony characteristics and cording (31), and the observed changes in colony morphology and cording in the Δ*kasB* mutant were thus likely a direct or indirect effect of the altered MA profile of the TDMs produced by the mutant. Loss of cording is often associated with decreased virulence (19), and indeed this was the case with the Δ*kasB* mutant. Before these studies, three other *M. tuberculosis* mutants defective in MA biosynthesis had been tested in the mouse model of infection: Δ*mma4* and Δ*pcaA* were found to be attenuated (16, 19), whereas Δ*cmaA2* was hypervirulent (32). Although Δ*pcaA* and Δ*mmaA4* showed reduced replication in mouse organs, moderately high numbers of bacteria could be found in the lungs, spleen, and liver of mice even 20–30 weeks after infection (albeit lower than those found for the WT strain) (16, 19). None of these three mutants has been reported as acid-fast negative, and only the Δ*pcaA* mutant was defective in cording.

The Δ*kasB* mutant displayed a number of interesting *in vivo* phenotypes. First, it was severely attenuated for growth in immunocompetent C57BL/6 mice: the mutant did initially colonize lung, liver, and spleen in infected immunocompetent C57BL/6 mice; determination of bacterial loads in organs and histological examination of tissue sections revealed that Δ*kasB* failed to replicate to the levels normally observed in these tissues and did not cause the pathology usually associated with *M. tuberculosis* infection.

Perhaps the most striking *in vivo* phenotype of the Δ*kasB* mutant was its ability to persist at constant low levels in lungs and spleen for 450 days after aerosol infection. The mutant also failed to cause active disease in the mice: Δ*kasB*-infected mice appeared healthy even 600 days after infection. In contrast, SCID mice succumbed to infection by Δ*kasB*, indicating a clear role for cell-mediated immunity in the control of replication of the Δ*kasB* mutant. The absence of any differences between WT and Δ*kasB* in regard to their ability to survive in macrophages suggests that early defense mechanisms, like intracellular oxidative damage in macrophages, did not play a role in the attenuation of the mutant strain. Thus, the surprising "hypovirulence" of Δ*kasB* could be a consequence of a number of other factors resulting from the altered MA profile and their effects on the interaction of the bacteria with the host adaptive immune system. One possibility is the exposure of cell envelope components, normally "masked" in WT strains, which may induce a more robust immune response. Another possibility is the modulation of the immune response by cell wall components; TDMs are the major cell wall glycolipids and are known to modulate the immune response (32, 33). It is therefore likely that Δ*kasB* TDMs containing altered MAs modulate innate and adaptive immune responses, resulting in the observed *in vivo* growth defect.

A third of the human population is latently infected with the tubercle bacillus, and this dormant, drug-tolerant stage of the bacterium is a major challenge for the tuberculosis therapy and control. Although this latency provides an important reservoir for disease reactivation, very little is known about bacterial and host factors that are involved in long-term persistence. The long-term persistence of Δ*kasB* for up to 600 days in immunocompetent mice without causing disease suggests that the mutant strain can provide a good model for studying latent *M. tuberculosis* infection. Furthermore, this unique *in vivo* phenotype makes *kasB* an attractive candidate for deletion in a live attenuated vaccine strain.

The increased sensitivity of the *kasB* mutant to lipophilic antibiotics highlights the attractiveness of KasB as an important secondary drug target in combination therapy. Specific inhibitors of KasB could be envisioned as inhibiting long-chain mero-MA biosynthesis and, as a result, attenuating *M. tuberculosis* while at the same time making the bacterium even more susceptible to drugs such as rifampicin used in combination. In addition to an increased permeability to lipophilic drugs, the increased sensitivity of Δ*kasB* to thiolactomycin, a drug known to inhibit both KasA and KasB (34), may have been due to a lesser titration of the drug as a result of the absence of KasB.

In summary, our studies have demonstrated that KasB-mediated elongation of MAs is crucial for cording, acid-fast staining, subsequent *trans*-cyclopropanation, and the ability of *M. tuberculosis* to cause disease in immunocompetent mice. Our findings have important implications for understanding and solving the problems of latency and antibiotic tolerance in *M. tuberculosis* infection.

Materials and Methods

Plasmids and Phages. Plasmids and phages used in this work are outlined in SI Table 2. Slow-growing mycobacteria were cultured in 7H9 broth (Difco, Sparks, MD) containing 10% Middlebrook OADC enrichment and 0.05% Tween 80, on 7H9 agar (made by adding 1.5% agar to OADC-enriched 7H9 broth), or on Middlebrook 7H10 agar (Difco). *Escherichia coli* strains were cultured in LB broth. The concentrations of antibiotics used were 75 μg/ml hygromycin and 20 μg/ml kanamycin for mycobacterial strains, and 150 μg/ml hygromycin and 40 μg/ml kanamycin for *E. coli*.

Construction of Deletion Mutants. For generating an allelic exchange construct designed to replace the *kasB* gene with a hygromycin resistance cassette (*hyg*), 500-bp sequences flanking the left and right of the *M. tuberculosis kasB* gene were PCR-amplified from pYUB2271 (a cosmid vector containing *kasB*) using the primer pairs MtKasB1 (5′-GCGACTAGTGGTAGGGCGATGACTCGC-3′) and MtKasB2 (5′-CGTATGCATACCAGCTCCGTCATTG-3′), and MtKasB3 (5′-GCGTCTAGAGAGATCGATTTGGACGTG-3′) and MtKasB4 (5′-GCAGGTACCACCGAGATCTGCGGGATG-3′), respectively. After cloning into pCR2.1-TOPO and sequencing, the cloned PCR fragments were excised by using the primer-introduced restriction sites and cloned into the allelic exchange plasmid vector pJSC347 (SI Table 2). The resultant plasmid, pYUB2417, was then packaged into the temperature-sensitive phage phAE159 (J. Kriakov and W.R.J., Jr., unpublished results), as described (35), to yield the *kasB*-knockout phage phAE404. Specialized transduction was performed as described (35).

Biochemical Analyses of MAs and Lipids. TLC analysis of MAs was done as described (23, 34). MA extraction and derivatization for TLC analysis, and purification for MS and NMR analysis, were

done as described (19, 36). In brief, MAs of each strain were liberated by alkali hydrolysis (10% KOH/methanol, wt/vol) from the heat-killed bacteria at 90°C for 2 h, followed by extraction with *n*-hexane. After methylation with diazomethane, each subclass, α-, methoxy-, and keto-MAME, was purified by preparative TLC of silica gel until a single spot was obtained. The developing system was benzene or *n*-hexane/diethyl ether (90:15, vol/vol). The molecular species of the MAMEs were detected by MALDI-TOF MS by using an Ultraflex II (Bruker Daltonics, Billerica, MA). The purified MAMEs were prepared in chloroform at a concentration of 1 mg/ml, and a droplet of a 1-μl sample was applied directly on the sample plate followed by 1 μl of matrix solution (2,5-dihydroxybenzoic acid/10 mg/ml in chloroform/methanol, 1:1 vol/vol). MAMEs were analyzed in the Reflectron mode with an accelerating voltage operating in positive mode of 20 kV. An external mass calibration was performed by peptide calibration standard II (Bruker Daltonics), including known peptide standards in a mass range from 700 to 4,000 Da (15). ^{1}H NMR spectra of MAMEs were obtained in $CDCl_3$ (100% D) by using a Bruker Avance 600 spectrometer at 25°C. Chemical shift values (in ppm) were relative to internal $CHCl_3$ resonance (at 7.26 ppm). Pyrolysis and subsequent GC-MS of MAs was done in accordance with published methods (37, 38). Lipid extraction and TLC analysis were done as described (39).

Mouse Infections. C57BL/6 mice were exposed to aerosols of different strains of *M. tuberculosis* in an aerosolization chamber. A suspension of 10^6 cfu/ml in PBS containing 0.05% Tween 80 and 0.004% antifoam was used as the inoculum to obtain ≈100 cfu per lung. Four mice from each infection group were killed 24 h after infection, and lung homogenates were plated on 7H9-agar plates to determine the efficiency of aerosolization. At different time points, three or four mice were killed from each infection group to determine bacterial loads in the spleen, lung, and liver. Eight mice from each group were also used to determine survival times of infected mice. Pathological analysis and histological staining of organ sections were done on tissues fixed in buffered 10% formalin.

We thank Annie Dai, Mei Chen, and John Kim for technical assistance; Jordan Kriakov (Albert Einstein College of Medicine) for providing phAE159; Howard Steinman for helpful comments; and Matsumi Doe, Shinji Maeda, and Takashi Naka of Osaka City University for technical support. This work was supported by Howard Hughes Medical Institute and National Institutes of Health Grants AI063537 (to W.R.J.) and AI26170 (to W.R.J., S.A.P and J.C.); Center for AIDS Research Grant AI051519; Grants H12-Shinko-30, H16-Shinko-1 and H18-Shinko-11 from the Ministry of Health, Labor, and Welfare in Japan (to N.F. and K.K.); a grant from the Medical Research Council and the Wellcome Trust, U.K. (to G.S.B.); and Centre National de la Recherche Scientifique CNRS ATIP "Microbiologie Fondamentale" (to L.K.). G.S.B. acknowledges support from Mr. James Bardrick in the form of a Personal Research Chair, and as a former Lister Institute-Jenner Research Fellow. A.B. acknowledges support from the Medical Research Council (U.K.) in the form of Career Development Award G0600105 at the University of Birmingham.

1. Trebucq A (2004) *Int J Tuberc Lung Dis* 8:805.
2. Bishop PJ, Neumann G (1970) *Tubercle* 51:196–206.
3. Neelsen F (1883) *Centralbl Med Wissen* 28:497.
4. Ziehl F (1882) *Deut Med Wochen* 8:451.
5. Goren MB, Cernich M, Brokl O (1978) *Am Rev Respir Dis* 118:151–154.
6. Harada K (1976) *Stain Technol* 51:255–260.
7. Murohashi T, Kondo E, Yoshida K (1969) *Am Rev Respir Dis* 99:794–798.
8. Koch-Weser D, Barclay WR, Ebert RH (1955) *Am Rev Tuberc* 71:556–565.
9. Besra GS, Sievert T, Lee RE, Slayden RA, Brennan PJ, Takayama K (1994) *Proc Natl Acad Sci USA* 91:12735–12739.
10. Brennan PJ, Nikaido H (1995) *Annu Rev Biochem* 64:29–63.
11. Cole ST, Brosch R, Parkhill J, Garnier T, Churcher C, Harris D, Gordon SV, Eiglmeier K, Gas S, Barry CE, III, *et al.* (1998) *Nature* 393:537–544.
12. Bhatt A, Kremer L, Dai AZ, Sacchettini JC, Jacobs WR, Jr (2005) *J Bacteriol* 187:7596–7606.
13. Gao LY, Laval F, Lawson EH, Groger RK, Woodruff A, Morisaki JH, Cox JS, Daffe M, Brown EJ (2003) *Mol Microbiol* 49:1547–1563.
14. Slayden RA, Barry CE, III (2002) *Tuberculosis* 82:149–160.
15. Dinadayala P, Laval F, Raynaud C, Lemassu A, Laneelle MA, Laneelle G, Daffe M (2003) *J Biol Chem* 278:7310–7319.
16. Dubnau E, Chan J, Raynaud C, Mohan VP, Laneelle MA, Yu K, Quemard A, Smith I, Daffe M (2000) *Mol Microbiol* 36:630–637.
17. Glickman MS (2003) *J Biol Chem* 278:7844–7849.
18. Glickman MS, Cahill SM, Jacobs WR, Jr (2001) *J Biol Chem* 276:2228–2233.
19. Glickman MS, Cox JS, Jacobs WR, Jr (2000) *Mol Cell* 5:717–727.
20. Takayama K, Wang C, Besra GS (2005) *Clin Microbiol Rev* 18:81–101.
21. Yuan Y, Barry CE, III (1996) *Proc Natl Acad Sci USA* 93:12828–12833.
22. Yuan Y, Crane DC, Musser JM, Sreevatsan S, Barry CE, III (1997) *J Biol Chem* 272:10041–10049.
23. Kremer L, Guerardel Y, Gurcha SS, Locht C, Besra GS (2002) *Microbiology* 148:3145–3154.
24. George KM, Yuan Y, Sherman DR, Barry CE, III (1995) *J Biol Chem* 270:27292–27298.
25. Watanabe M, Aoyagi Y, Ridell M, Minnikin DE (2001) *Microbiology* 147:1825–1837.
26. Astola J, Munoz M, Sempere M, Coll P, Luquin M, Valero-Guillen PL (2002) *Microbiology* 148:3119–3127.
27. Watanabe M, Ohta A, Sasaki S, Minnikin DE (1999) *J Bacteriol* 181:2293–2297.
28. Veyron-Churlet R, Bigot S, Guerrini O, Verdoux S, Malaga W, Daffe M, Zerbib D (2005) *J Mol Biol* 353:847–858.
29. Veyron-Churlet R, Guerrini O, Mourey L, Daffe M, Zerbib D (2004) *Mol Microbiol* 54:1161–1172.
30. Walters SB, Dubnau E, Kolesnikova I, Laval F, Daffe M, Smith I (2006) *Mol Microbiol* 60:312–330.
31. Hunter RL, Venkataprasad N, Olsen MR (2006) *Tuberculosis* 86:349–356.
32. Rao V, Gao F, Chen B, Jacobs WR, Jr, Glickman MS (2006) *J Clin Invest* 116:1660–1667.
33. Rao V, Fujiwara N, Porcelli SA, Glickman MS (2005) *J Exp Med* 201:535–543.
34. Kremer L, Douglas JD, Baulard AR, Morehouse C, Guy MR, Alland D, Dover LG, Lakey JH, Jacobs WR, Jr, Brennan PJ, *et al.* (2000) *J Biol Chem* 275:16857–16864.
35. Bardarov S, Bardarov S, Jr, Pavelka MS, Jr, Sambandamurthy V, Larsen M, Tufariello J, Chan J, Hatfull G, Jacobs WR, Jr (2002) *Microbiology* 148:3007–3017.
36. Fujiwara N, Pan J, Enomoto K, Terano Y, Honda T, Yano I (1999) *FEMS Immunol Med Microbiol* 24:141–149.
37. Guerrant GO, Lambert MA, Moss CW (1981) *J Clin Microbiol* 13:899–907.
38. Kaneda K, Imaizumi S, Yano I (1995) *Microbiol Immunol* 39:563–570.
39. Dobson G, Minnikin DE, Minnikin SM, Parlett M, Goodfellow M, Ridell M, Magnusson M (1985) in *Chemical Methods in Bacterial Systematics*, eds Goodfellow M, Minnikin DE (Academic, London), pp 237–265.

Letters in Applied Microbiology ISSN 0266-8254

ORIGINAL ARTICLE

The first molecular analysis of clinical isolates of VanA-type vancomycin-resistant *Enterococcus faecium* strains in Mainland China

B. Zheng[1,2], H. Tomita[2], Y.H. Xiao[1] and Y. Ike[2,3]

1 Institute of Clinical Pharmacology, Peking University First Hospital, Beijing, China
2 Department of Bacteriology and Bacterial Infection Control, Gunma University Graduate School of Medicine, Maebashi, Gunma, Japan
3 Laboratory of Bacterial Drug Resistance, Gunma University Graduate School of Medicine, Maebashi, Gunma, Japan

Keywords
China, *Enterococcus faecium*, insertion sequence, Tn*1546*-like element, VanA-type, vancomycin-resistant *Enterococcus faecium*.

Correspondence
H. Tomita, Department of Bacteriology and Bacterial Infection Control, Gunma University Graduate School of Medicine, Showa-machi 3-39-22, Maebashi, Gunma 371-8511, Japan.
E-mail: tomitaha@med.gunma-u.ac.jp

2006/0256: received 24 February 2006, revised 2 March 2007 and accepted 26 April 2007

doi:10.1111/j.1472-765X.2007.02191.x

Abstract

Aims: The aim of this study was to examine two VanA-type vancomycin-resistant *Enterococcus faecium* (VRE) strains that had been isolated from patients resident in mainland China. This is the first molecular analysis of clinical VRE strains being isolated in mainland China.

Methods and Results: Two VanA-type VRE isolates were isolated from in-patients at hospitals located in the Chinese cities Beijing and Dalian and were designated C264 and I125. The plasmids pC264V (40 kbp) and pI125V (370 kbp) that were isolated from C264 and I125, respectively, carried a Tn*1546*-like element encoding VanA resistance. The vancomycin-resistant plasmids pC264V and pI125V were transferred by filter mating at frequencies of 10^{-7} and 10^{-4} respectively. Sequence analysis of pC264V revealed that two IS*1216V* sequences and an IS*1542* sequence were present within the Tn*1546*-like element. pI125V had two IS*1216V* insertions in the Tn*1546*-like element.

Conclusions: The two VanA-type vancomycin-resistant *E. faecium* (VRE) strains C264 and I125 were isolated from in-patients in Chinese hospitals. The vancomycin-resistant conjugative plasmids pC264V and pI125V plasmids isolated from these strains carried the Tn*1546*-like element. The Tn*1546*-like element was found to contain the insertion sequences IS*1216V* and IS*1542*.

Significance and Impact of the Study: This is the first molecular analysis of VanA-type VRE strains from patients resident in mainland China.

Introduction

The first cases of the isolation of vancomycin-resistant enterococci (VRE) were reported in 1988 in the United Kingdom (Uttley *et al.* 1988) and France (Leclercq *et al.* 1988), and shortly thereafter, VRE was detected in hospitals in the United States (Sahm *et al.* 1989). Since then, VRE have emerged with unanticipated rapidity and are now encountered in many hospitals, particularly in the United States (Martone 1998; Cetinkaya *et al.* 2000).

There have been a number of reports describing the isolation of VRE in East Asian countries such as Japan, Korea and Taiwan. The frequency of VRE isolation from both patients and food animals is increasing in Korea and Taiwan (Kim and Song 1998; Lu *et al.* 2001; Lauderdale *et al.* 2002; Yu *et al.* 2003; Song *et al.* 2005). Japan has also seen an increase in the frequency of VRE isolation from patients (Ike *et al.* 1999; Ozawa *et al.* 2002) since the first report of a VanA-type VRE (*E. faecium*) clinical isolate in 1996 (Fujita *et al.* 1998).

Vancomycin has been used for more than 30 years in China, but to date there has been few reports describing the isolation of clinical VRE strains and no molecular analysis of VRE strains in this country (Wang 2006). We believe this is the first molecular analysis of clinical VanA-type VRE strains in mainland China. In this report,

we describe the molecular analysis of the Tn*1546*-like elements present in the VRE isolates.

Materials and methods

Bacterial strains, media and antibiotics

The vancomycin-resistant *Enterococcus faecium* (VRE) strains C264 and I125 were isolated from in-patients resident at two different hospitals in China in 2001 and 2003 respectively. *Enterococcus faecalis* FA2-2 (Clewell *et al.* 1982), which is rifampicin and fusidic acid resistant, was used as a recipient in the mating experiments. Todd–Hewitt broth (Difco, Detroit, MI, USA) was used as the growth medium for enterococci. Mueller–Hinton (MH) broth and MH agar (Nissui, Tokyo, Japan) were used in the sensitivity assays to test the antibiotic minimal inhibitory concentrations (MICs).

MIC determination

The MICs were determined by the agar dilution method according to the criteria set by the National Committee for Clinical Laboratory Standards (2000) using MH agar.

Mating procedures

Filter mating was performed with a donor/recipient ratio of 1 : 10 (Franke and Clewell 1981). Broth mating was performed as previously described with a donor/recipient ratio of 1 : 10 (Dunny *et al.* 1979). The conjugative transfer frequency was calculated as the ratio of the number of transconjugants to the number of donors.

Isolation and manipulation of plasmid DNA

Plasmid DNA was isolated by the alkaline lysis method (Sambrook *et al.* 1989). Restriction enzymes were obtained from New England Biolabs, Inc. (Beverly, MA, USA) and Takara Bio Inc., (Tokyo, Japan).

DNA sequencing analysis of Tn*1546*-like elements

The DNA fragments to be sequenced were amplified by PCR using the thermostable DNA polymerase TaKaRa *Taq* (Takara Bio Inc.) and a Perkin-Elmer 9600 thermal cycler (Applied Biosystems, Foster City, CA, USA). The PCR conditions were varied according to the primers used and the size of the anticipated product. The custom primers used in this study were obtained from Invitrogen (Tokyo, Japan). The sequencing reaction was carried out with a Dye Terminator Cycle Sequencing FS ready Reaction Kit (Perkin-Elmer). The nucleotide sequence was determined using an ABI PRISM 310 genetic analyser and 377 DNA sequencer (Perkin-Elmer).

Pulsed-field gel electrophoresis

Cells were pretreated with 20 mg ml^{-1} of lysozyme for 2 h and then lysed in an agarose plug according to the standard protocol (Sambrook *et al.* 1989). The agarose plugs were then placed in 300 μl of reaction mixture containing 50 U of *Sma*I to digest total DNA. The gels were electrophoresed with a clamped homogeneous electric field (6 V cm^{-1}, 15°C for 24 h, Switch times ramped from 1 to 25 s; CHEF-DR II; Bio-Rad Laboratories, Richmond, CA, USA).

DNA–DNA Southern hybridization

Southern hybridization was carried out with the digoxigenin-based nonradioisotope system of Boehringer GmbH (Mannheim, Germany), and all procedures were based on the manufacturer's manual and standard protocols (Sambrook *et al.* 1989). The PCR product specific for *vanA* was used to construct a probe for the detection of the *vanA* gene. Signals were detected using nitroblue tetrazolium-5-bromo-4-chloro-3-indolylphosphate stock solution (Roche Diagnostics GmbH, Mannheim, Germany).

Results

Isolation of two VRE strains

The two VRE strains C264 and I125 were isolated from in-patients resident at two different hospitals in 2001 and 2003 respectively. C264 was isolated from bile exudates obtained from a 50-year-old male patient hospitalized in a Beijing hospital who was suffering from progressive gastric cancer with systemic metastasis. The infectious bile exudates were isolated from the percutaneous choledochal drainage tube being used in the treatment of obstructive jaundice caused by the metastasis. Prior to isolation of C264, the patient had been treated with cefoperazone/sulbactam (2·0 g day^{-1} for a total of 32 days), ceftazydime (2·0 g day^{-1} for 4 days) and clindamycin (0·6 g day^{-1} for 3 days). I125 was isolated from sputum obtained from a 45-year-old male patient who had been hospitalized in a Dalian hospital for the treatment of hepatocirrhosis after having undergone a liver transplant. The patient had contracted pneumonia while in the hospital and had been treated with vancomycin (0·5 g day^{-1} for 5 days), cefepime (1·0 g day^{-1} for 3 days) and cefoperazone/sulbactam (2·0 g day^{-1} for 6 days) prior to the isolation of the I125 strain.

Table 1 MICs of the vancomycin-resistant *Enterococcus faecium* isolates ($\mu g \cdot ml^{-1}$)

Drug	C264	I125
Ampicillin	256	64
Imipenem	512	512
Gentamicin	512	512
Erythromycin	512	512
Ofloxacin	64	64
Moxifloxacin	16	8
Gatifloxacin	16	8
Tetracycline	0·5	0·5
Vancomycin	128	32
Teicoplanin	32	32

MIC, minimal inhibitory concentration.

Characterization of the strains

The drug resistance levels (MICs, in $\mu g\ ml^{-1}$) for C264 and I125 are shown in Table 1. C264 has a relatively high-level MIC for vancomycin (128 $\mu g\ ml^{-1}$) and I125 has an intermediate-level MIC for vancomycin (32 $\mu g\ ml^{-1}$). Both isolates have an intermediate level of resistance to teicoplanin (32 $\mu g\ ml^{-1}$ in MIC). The vancomycin resistance genes of the isolates were examined by PCR amplification using specific primers for the reported *van* genes. In both cases, amplified *vanA*-specific products were detected and confirmed by DNA sequencing (data not shown). The pulsed-field gel electrophoresis (PFGE) profiles of *Sma*I-digested chromosomal DNA from C264 and I125 differed from one another and no relationship between the two strains was detected (Fig. 1a).

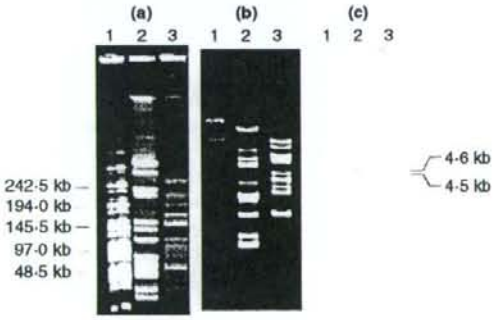

Figure 1 Pulsed-field gel electrophoresis (PFGE) of *Sma*I-digested chromosomal DNAs from vancomycin-resistant *Enterococcus faecium* isolates, C264 and I125 (a). Agarose gel electrophoresis of the *Eco*RI-digested plasmid DNAs from *E. faecium* C264 and I125 isolates (b) and Southern hybridization analysis using *vanA* probe (c). Lane 1: molecular weight markers (a) Midrange PFG marker (New England Biolabs), (b and c) *Hin*dIII-digested lambda DNA; Lane 2: C264; Lane3: I125.

Transferability of vancomycin resistance and the vancomycin-resistant plasmids

The transfer of vancomycin resistance by broth mating and by filter mating was examined in the two VRE isolates. The vancomycin resistances of C264 and I125 only transferred to *E. faecalis* FA2-2 strains by filter mating at frequencies of 10^{-7} and 10^{-4} per donor cell respectively.

*Eco*RI-digested plasmid DNA prepared from C264 and I125 showed that both strains harbored several plasmids (Fig. 1b). The plasmid DNAs were examined by Southern hybridization analysis using the *vanA* probe (Fig. 1c). The *vanA* probe hybridized to a 4·6 kbp *Eco*RI fragment of plasmid DNA obtained from C264 and a 4·5 kbp *Eco*RI fragment of plasmid DNA obtained from I125. The intensity of the 4·5 kbp band of I125 was relatively faint compared with that of the 4·6 kbp band of C264 on the Southern blot membrane (Fig. 1c).

To confirm that the *vanA* gene of I125 was encoded on the plasmid, the vancomycin-resistant transconjugant of *E. faecalis* FA2-2 obtained in the mating experiment with I125 was examined in detail. Plasmid DNA prepared from the transconjugant FA2-2/I125V was too faint to detect clearly on the agarose gel. Undigested total DNA prepared from FA2-2/I125V was separated by PFGE and the gel was then Southern blotted and hybridized with the *vanA* probe (data not shown). A 370 kbp DNA fragment had migrated from the well and was detected on the agarose gel. The DNA band appeared to result from nonspecific digestion of the plasmid, and the *vanA* probe hybridized to this band. These data indicated that the *vanA* gene was encoded on the large conjugative plasmid designated as pI125V (370 kbp). PFGE and Southern hybridization detection of the *vanA* gene were performed using C264 and the results showed that the vancomycin resistance was encoded on a 40 kbp conjugative plasmid designated as pC264V.

Structure of the Tn*1546*-like elements

The DNA sequences of the Tn*1546*-like elements encoding the *vanA*-operon were determined for the vancomycin resistance genes encoded on the plasmid pI125V and pC264V. Overlapping internal fragments of the Tn*1546*-like element carried by each plasmid were amplified using the specific primer sets and each amplified PCR product was sequenced and compared with the reported prototype Tn*1546* element (10 851 bp) carried by pIP816 (34 kbp) of *E. faecium* BM4147 (Fig. 2) (Arthur *et al.* 1993). Specific primers for the insertion sequences IS*1216V* (809 bp) and IS*1542* (1324 bp), which are often found in the Tn*1546*-like element, were also used in sequence analysis (Handwerger and Skoble 1995; Woodford *et al.* 1998).

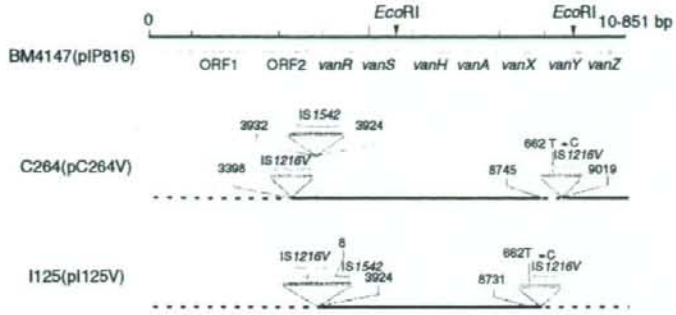

Figure 2 Genetic map and organization of the Tn*1546*-like elements of C264, I125 and the prototype element found in *Enterococcus faecium* BM4147. The upper horizontal arrows show the genes and open reading frames (ORFs) encoded on the prototype Tn*1546* element of plasmid pIP816. Boxes with vertical lines represent insertion sequence (IS) elements. The numbers at the IS insertions show the positions of the first nucleotides upstream and downstream of the inserts. The horizontal arrows on the IS elements indicate the transcriptional orientation of transposase encoded on the ISs. The dotted horizontal lines indicate the deleted region.

The sequence data obtained by analysis of the Tn*1546*-like elements of the plasmids and their comparison with the prototype element are shown in Fig. 2. Sequence analysis of pC264V revealed that the IS*1216V* sequences had inserted into open reading frames 2 (ORF2) upstream of *vanR* and into the internal region between *vanX* and *vanY* of the Tn*1546*-like element of pC264V, and an IS*1542* sequence had inserted into the internal region between ORF2 and the *vanR* gene. IS*1216V* had inserted at 366 bp, and the region upstream of 365 bp in the N-terminal region of ORF2 (576 bp) had been deleted in the Tn*1546*-like element. The deleted region contained ORF1 and the 365 bp N-terminal region of ORF2 of the Tn*1546*-like element. The 273 bp segment upstream of the IS*1216V* insertion within the internal region between *vanX* and *vanY* was also deleted. IS*1542* had inserted at position 3932 bp of Tn*1546* within an 8 bp-duplication that might correspond to the 'CTATAATC' target sequence. pI125V had two IS*1216V* insertions in the Tn*1546*-like element. One IS*1216V* element had inserted at 52 bp in the region upstream of *vanR*. The region upstream of the insertion, where ORF1 and ORF2 were located, had been deleted. Another IS*1216V* had inserted into the internal region between *vanX* and *VanY* and the region downstream of the insertion, where *vanY* and *vanZ* were located, was also deleted. Both plasmids had a nucleotide substitution from T to C at position 662 bp in the IS*1216V* located in the internal region between *vanX* and *vanY* (Fig. 2). The nucleotide substitution did not result in any amino acid substitution in the deduced amino acid sequences of the transposase (228 aa) encoded on IS*1216V*.

Discussion

Vancomycin has been used for about 40 years in the treatment of patients in mainland China, but there has been no report to date describing the isolation of clinical VRE strains. The two VanA-type VRE strains, C264 and I125, are the first clinical isolates of Chinese origin to be reported. The PFGE profiles indicated that they were unrelated, although both carried vancomycin-resistant conjugative plasmids and had insertion sequences in the Tn*1546*-like elements. The *vanS* genes of pC264V and pI125V were identical to that of the BM4147 strain and there were no substitutions in the gene. The resistance levels differed from VanA-type VRE strains that have three substitutions within VanS resulting in low-level teicoplanin resistance, which are frequently isolated in Japan from chicken meat imported from Thailand (Hashimoto *et al.* 2000; Ozawa *et al.* 2002) and are also found in Taiwanese VRE (Lauderdale *et al.* 2002). Recently, a VanA-type *Enterococcus faecalis* strain was isolated from chicken meat imported from China and was described by our group (Tanimoto *et al.* 2005). The isolate harboured the vancomycin-resistance conjugative plasmid and three substitutions within VanS identical to those found in the Thai chicken VRE isolates. Our data showed that the origins of the Chinese clinical VRE isolates differed from that of the VRE isolate obtained from Chinese chicken meat.

Insertion sequences such as IS*1216V* and IS*1542* are frequently found in the Tn*1546*-like elements of VanA-type VRE isolates and partial deletion of DNA is also common (Jensen 1998; Palepou *et al.* 1998; Willems *et al.* 1999; Yu *et al.* 2003). Our sequence analysis showed that

the insertion sequences and deletions were found in the Tn*1546*-like elements of pC264V and pI125V. We were unable to determine why the I125 isolate showed an intermediate level of resistance to vancomycin (MIC; 32 $\mu g\ ml^{-1}$) in this study, but some reports explain the decline in MIC as a result of insertions or deletions within *vanX* and *vanY* , as we had observed in the sequence of pI125V (Lee *et al.* 2004; Naas *et al.* 2005). IS*1542* had inserted at 3932 bp within the pC264V Tn*1546*, within an 8 bp-duplication that might correspond to the 'CTATAATC' target sequence. The target site within the pC264V Tn*1546*-like element was identical to the insertion sites in VanA-type VRE isolates seen in Europe and Korea (Schouten *et al.* 2001; Huh *et al.* 2004; Lee *et al.* 2004). These data imply that the Tn*1546* element has a hot spot sequence for the insertion of IS*1542*. Eight base pair sequences identical to the end of IS*1542* were found between the IS*1216V* sequences and position 3924 bp of Tn*1546* in pI125V, suggesting that IS*1542* had inserted into the Tn*1546* hot spot and then at a later time IS*1216V* had inserted into the IS*1542* (Fig. 2). Both plasmids had a T to C nucleotide substitution at 662 bp in the IS*1216V* in the internal region between *vanX* and *vanY*. The origins of the IS*1216V*s carrying a one base pair substitution might differ from those of the other IS*1216V*s that had no substitution and were located in the upstream region of the Tn*1546*-like element.

Although these VanA-type VRE strains were isolated independently in China, the distribution and insertion of IS*1216V* and IS*1542* associated with the Tn*1546*-like elements of the Chinese isolates were similar to the European and Korean VanA-type VRE isolates that have been previously reported (Willems *et al.* 1999; Darini *et al.* 2000; Schouten *et al.* 2001; Yu *et al.* 2003; Huh *et al.* 2004; Lee *et al.* 2004). In order to understand the characteristics of Chinese VanA-type VRE strains, a nationwide surveillance of VRE would be required as would further analyses of other VanA-type VRE.

Acknowledgements

This study was supported by grants from the Japanese Ministry of Education, Culture, Sport, and Science and Technology [Tokuteiryoiki (C), Kiban (B), Kiban (C)], and the Japanese Ministry of Health, Labor and Welfare (H15-Shinko-9). We thank Dr. Elizabeth Kamei for revising the manuscript.

References

Arthur, M., Molinas, C., Depardieu, F. and Courvalin, P. (1993) Characterization of Tn*1546*, a Tn*3*-related transposon conferring glycopeptide resistance by synthesis of depsipeptide peptidoglycan precursors in *Enterococcus faecium* BM*4147*. *J Bacteriol* **175**, 117–127.

Cetinkaya, Y., Falk, P. and Mayhall, C.G. (2000) Vancomycin-resistant enterococci. *Clin Microbiol Rev* **13**, 686–707.

Clewell, D., Tomich, P., Gawron-Bruke, M., Franke, A.E., Yagi, A. and An, F. (1982) Mapping of *Streptococcus faecalis* plasmids pAD1 and pAD2 and studies relating to transposition of Tn*917*. *J Bacteriol* **152**, 1220–1230.

Darini, A.L., Palepou, M.F. and Woodford, N. (2000) Effects of the movement of insertion sequences on the structure of VanA glycopeptide resistance elements in *Enterococcus faecium*. *Antimicrob Agents Chemother* **44**, 1362–1364.

Dunny, G.M., Craig, R.A., Carron, R.L. and Clewell, D.B. (1979) Plasmid transfer in *Streptococcus faecalis*: production of multiple sex pheromones by recipients. *Plasmid* **2**, 454–465.

Franke, A.E. and Clewell, D.B. (1981) Evidence for a chromosome-borne resistance transposon (Tn*916*) in *Streptococcus faecalis* that is capable of "conjugal" transfer in the absence of a conjugative plasmid. *J Bacteriol* **145**, 494–502.

Fujita, N., Yoshimura, M., Komori, T., Tanimoto, K. and Ike, Y. (1998) First report of the isolation of high-level vancomycin-resistant *Enterococcus faecium* from a patient in Japan. *Antimicrob Agents Chemother* **42**, 2150.

Handwerger, S. and Skoble, J. (1995) Identification of chromosomal mobile element conferring high-level vancomycin resistance in *Enterococcus facium*. *Antimicrob Agents Chemother* **39**, 2446–2453.

Hashimoto, Y., Tanimoto, K., Ozawa, Y., Murata, T. and Ike, Y. (2000) Amino acid substitutions in the VanS sensor of the VanA-type vancomycin-resistant *Enterococcus* strains results in high-level vancomycin resistance and low-level teicoplanin resistance. *FEMS Microbiol Lett* **185**, 247–254.

Huh, J.Y., Lee, W.G., Lee, K., Shin, W.S. and Yoo, J.H. (2004) Distribution of insertion sequences associated with Tn*1546*-like elements among *Enterococcus faecium* isolates from patients in Korea. *J Clin Microbiol* **42**, 1897–1902.

Ike, Y., Tanimoto, K., Ozawa, Y., Nomura, T., Fujimoto, S. and Tomita, H. (1999) Vancomycin-resistant enterococci in imported chickens in Japan. *Lancet* **353**, 1854.

Jensen, L.B. (1998) Internal size variations in Tn*1546*-like elements due to the presence of IS*1216V*. *FEMS Microbiol Lett* **169**, 349–354.

Kim, J.M. and Song, Y.G. (1998) Vancomycin-resistant enterococcal infections in Korea. *Yonsei Med J* **39**, 562–568.

Lauderdale, T.L., McDonald, L.C., Shiau, Y.R., Chen, P.C., Wang, H.Y., Lai, J.F. and Ho, M. (2002) Vancomycin-resistant enterococci from humans and retail chickens in Taiwan with unique VanB phenotype-*vanA* genotype incongruence. *Antimicrob Agents Chemother* **46**, 525–527.

Leclercq, R., Derlot, E., Duval, J. and Courvalin, P. (1988) Plasmid-mediated resistance to vancomycin and teicoplanin in *Enterococcus faecium*. *N Engl J Med* **319**, 157–161.

Lee, W.G., Hun, J.Y., Cho, S.R. and Lim, Y.A. (2004) Reduction in glycopeptide resistance in vancomycin-resistant

enterococci as a result of *vanA* cluster rearrangements. *Antimicrob Agents Chemother* **48**, 1379–1381.

Lu, J.J., Perng, C.L., Chiueh, T.S., Lee, S.Y., Chen, C.H., Chang, F.Y., Wang, C.C. and Chi, W.M. (2001) Detection and typing of vancomycin-resistance genes of enterococci from clinical and nosocomial surveillance specimens by multiplex PCR. *Epidemiol Infect* **126**, 357–363.

Martone, W.J. (1998) Spread of vancomycin resistant enterococci: why did it happen in the United States? *Infect Control Hosp Epidemiol* **19**, 539–545.

Naas, T., Fortineau, N., Snanoudj, R., Spicq, C., Durrbach, A. and Nordmann, P. (2005) First nosocomial outbreak of vancomycin-resistant *Enterococcus feacium* expressing a VanD-like phenotype associated with vanA genotype. *J Clin Microbiol* **43**, 3642–3649.

Ozawa, Y., Tanimoto, K., Nomura, T., Yoshinaga, M., Arakawa, Y. and Ike, Y. (2002) Vancomycin-resistant enterococci in humans and imported chickens in Japan. *Appl Environ Microbiol* **68**, 6457–6461.

Palepou, M.F., Adebiyi, A.M., Tremlett, C.H., Jensen, L.B. and Woodford, N. (1998) Molecular analysis of diverse elements mediating VanA glycopeptide resistance in enterococci. *J Antimicrob Chemother* **42**, 605–612.

Sahm, D.F., Kissinger, J., Gilmore, M.S., Murray, P.R., Mulder, R., Solliday, J. and Clarke, B. (1989) *In vitro* susceptibility studies of vancomycin-resistant *Enterococcus faecalis*. *Antimicrob Agents Chemother* **33**, 1588–1591.

Sambrook, J., Fritsch, E.F. and Maniatis, T. (1989) *Molecular Cloning: A Laboratory Manual*, 2nd edn. Cold Spring Harbor, NY: Cold Spring Harbor Laboratory Press.

Schouten, M.A., Willems, R.J., Kraak, W.A., Top, J., Hoogkamp-Korstanje, J.A. and Voss, A. (2001) Molecular analysis of Tn*1546*-like elements in vancomycin-resistant enterococci isolated from patients in Europe shows geographic transposon type clustering. *Antimicrob Agents Chemother* **45**, 986–989.

Song, J.Y., Hwang, I.S., Eom, J.S., Cheong, H.J., Bae, W.K., Park, Y.H. and Kim, W.J. (2005) Prevalence and molecular epidemiology of vancomycin-resistant enterococci (VRE) strains isolated from animals and humans in Korea. *Korean J Intern Med* **20**, 55–62.

Tanimoto, K., Nomura, T., Hamatani, H., Xiao, Y.H. and Ike, Y. (2005) A vancomycin-dependent VanA-type *Enterococcus faecalis* strain isolated in Japan from chicken imported from China. *Lett Appl Microbiol* **41**, 157–162.

Uttley, A.H., Collins, C.H., Naidoo, J. and George, R.C. (1988) Vancomycin-resistant enterococci. *Lancet* **1**, 57–58.

Wang, F. (2006) CHINET 2005 surveillance of bacterial resistance in China. *Chinese J Infect Chemother* **6**, 289–295.

Willems, R.J., Top, J., van den Braak, N., van Belkum, A., Mevius, D.J., Hendriks, G., van Santen-Verheuvel, M. and van Embden, J.D. (1999) Molecular diversity and evolutionary relationships of Tn*1546*-like elements in enterococci from humans and animals. *Antimicrob Agents Chemother* **43**, 483–491.

Woodford, N., Anebiyi, A.M., Palepou, M.F. and Cookson, B.D. (1998) Diversity of VanA glycopeptide resistance elements in enterococci from humans and nonhuman sources. *Antimicrob Agents Chemother* **42**, 502–508.

Yu, H.S., Seol, S.Y. and Cho, D.T. (2003) Diversity of Tn*1546*-like elements in vancomycin-resistant enterococci isolated from humans and poultry in Korea. *J Clin Microbiol* **41**, 2641–2643.

Evaluation of major membrane protein-II as a tool for serodiagnosis of leprosy

Yumi Maeda[1], Tetsu Mukai[1], Masanori Kai[1], Yasuo Fukutomi[1], Hiroko Nomaguchi[1], Chiyoji Abe[3], Kazuo Kobayashi[4], Seigo Kitada[5], Ryoji Maekura[5], Ikuya Yano[6], Norihisa Ishii[2], Toru Mori[1,2] & Masahiko Makino[1]

[1]Department of Microbiology, Leprosy Research Center, National Institute of Infectious Diseases, Tokyo, Japan; [2]Department of Bioregulation, Leprosy Research Center, National Institute of Infectious Diseases, Tokyo, Japan; [3]Research Institute of Tuberculosis, Tokyo, Japan; [4]Department of Host Defense, Graduate School of Medicine, Osaka City University, Osaka, Japan; [5]Department of Internal Medicine, Toneyama National Hospital, Osaka, Japan; and [6]Japan BCG Central Laboratory, Kiyose, Tokyo, Japan

Correspondence: Yumi Maeda, Department of Microbiology, Leprosy Research Center, National Institute of Infectious Diseases (NIID), 4-2-1 Aobacho, Higashimurayama, Tokyo 189-0002, Japan. Tel.: +81 42 391 8211; fax: +81 42 391 8212; e-mail: yumi@nih.go.jp

Received 24 January 2007; revised 3 April 2007; accepted 10 April 2007.
First published online 22 May 2007.

DOI:10.1111/j.1574-6968.2007.00754.x

Editor: Roger Buxton

Keywords
serology; diagnosis; infection; mycobacteria; leprosy.

Abstract

As serodiagnosis is the easiest way of diagnosing a disease, the utility of *Mycobacterium leprae*-derived major membrane protein-II (MMP-II), one of the immuno-dominant antigens, in the serodiagnosis of leprosy was examined. The percent positivity by an enzyme-linked immunosorbent assay for anti-MMP-II antibody was 82.4% for multi-bacillary leprosy, and the specificity of the test was 90.1%. For pauci-bacillary leprosy where cell-mediated immunity predominates, 39.0% showed positive results. These percentage values were significantly higher than these values obtained for existing phenolic glycolipid-I based methods, suggesting that MMP-II antibody detection would facilitate the diagnosis of leprosy.

Introduction

Leprosy represents a broad-spectrum disease caused by *Mycobacterium leprae*, with lepromatous leprosy at one pole and tuberculoid leprosy at the other end of the pole, depending on the clinical manifestation, which is an ultimate effect of the immunity of the host (Ridley & Jopling, 1996). In all forms of the disease, *M. leprae* induces skin lesions and a chronic progressive peripheral nerve injury, to a lesser or greater extent, which leads to systemic deformity (Stoner, 1979; Job, 1989). Therefore, early detection of *M. leprae* infection is the key to avoiding deformities. The diagnosis of leprosy is based on microscopic detection of acid-fast bacteria (AFB) in skin smears or biopsies, along with clinical and histopathological evaluation. Acid-fast staining requires at least a thousand organisms per gram of tissue for reliable detection (Shepard & McRae, 1968), resulting in an extremely low sensitivity, especially for the tuberculoid form of the disease, where AFB are rare or absent. Recently, real-time PCR-based methods have been developed (Martinez *et al.*, 2006), but the sensitivity of the test for clinical specimens is still problematic. In developing countries, where leprosy is endemic, diagnosis still relies on clinical observations and easy inexpensive tests. Serodiagnosis is the most easy and tangible way of diagnosing a disease. For leprosy, the only antigen currently used is phenolic glycolipid-I (PGL-I), which is supposed to be *M. leprae* specific. Since the discovery of PGL-I in 1981 by Hunter and Brennan, considerable progress has been made in the development of serological tools (Hunter & Brennan, 1981). In this process, simple user-friendly assays such as Serodia leprae®, a simple lateral flow test, and dipstick assays, based on PGL-I antigen, have been developed to detect leprosy patients in leprosy-endemic areas (Izumi *et al.*, 1990; Buhrer-Sekula *et al.*, 2003). However, these tests seem to be insufficient to detect both multi-bacillary and pauci-bacillary patients, as well as for early diagnosis, and have not been used as widely as would be expected, in the field situations. Therefore, there is a need to look for more sensitive

antigens. To date, various antigens of *M. leprae* have been studied (Hunter *et al.*, 1990), but due to a lack of either specificity or sensitivity, their use has been limited. Major membrane protein-II (MMP-II, #ML2038c, gene name bfrA, also known as bacterioferritin) had been identified previously from the cell membrane fraction of *M. leprae* as an antigenic molecule capable of activating both antigen-presenting cells and T cells (Pessolani *et al.*, 1994; Maeda *et al.*, 2005). These findings prompted examination of the role of MMP-II in the humoral responses of patients. Here, MMP-II was expressed and purified in *Escherichia coli* and the use of MMP-II as an antigen for the serodiagnosis of leprosy was evaluated.

Materials and methods

Study population

Sera were obtained with informed consent from healthy individuals, leprosy patients, and tuberculosis patients from Japan. The samples were frozen at $-30\,^{\circ}C$ before use. The population studied included multi-bacillary ($n=74$) and pauci-bacillary ($n=77$) leprosy patients, either treated or untreated, from the National Sanatorium Oshimaseishoen, and tuberculosis patients ($n=55$) from Fukujuji Hospital. Classification of leprosy was performed according to WHO recommendations. The home page is available at http://www.who.int/lep/classification/en/index.html. Individuals who have not been vaccinated with *Mycobacterium bovis* bacillus Calmette–Guerin (BCG) are unavailable in Japan, due to compulsory vaccination at least once in childhood. Therefore, sera from BCG-vaccinated healthy volunteers ($n=81$) residing in Japan were used as negative controls in the enzyme-linked immunosorbent assay (ELISA) to determine the cut-off value for positivity. The age and sex of normal individuals may not be fully matched with those of patients because some of the details of leprosy patients as well as normal individuals are unknown. This study was approved by the ethics committee of the National Institute of Infectious Diseases, Tokyo.

Expression and purification of protein

The MMP-II gene (ML2038c, *bfr*A) was expressed in *E. coli* as a fusion construct using a pMAL-c2X expression vector (New England BioLabs). The protein was affinity purified to almost homogeneity using an amylose column (data not shown), and used as the antigen for the detection of anti-MMP-II antibody levels in the leprosy patients. The synthetic bovine serum albumin (BSA)-conjugated trisaccharide-phenyl propionate (NTP-BSA) for the detection of PGL-I antibodies was kindly provided by Dr T. Fujiwara, Institute for Natural Sciences, Nara University. The procedure for synthesis of the antigen is described elsewhere (Fujiwara *et al.*, 1984).

Assay method for the detection of antibodies

The ELISA for the detection of anti-MMP-II immunoglobulin G (IgG) antibodies or anti-PGL-I IgM antibodies was performed as described previously, with modifications (Izumi *et al.*, 1990). Ninety-six well plates (Immunosorb, Nunc) were coated overnight, with MMP-II at a concentration of $2\,\mu g\,mL^{-1}$ in 0.1 M carbonate buffer (pH 9.5). After blocking with 2% skim milk, the plates were washed with phosphate-buffered saline containing 0.1% Tween 20 (PBST), and human sera (normal or patient's sera) diluted 100-fold were added and incubated at 37 °C for 2 h. After washing with PBST, biotinylated anti-human IgG (Vector Laboratories) was added at a concentration of $0.5\,\mu g\,mL^{-1}$ and incubated for 1 h. The plates were incubated with reagents from a Vectastain ABC Kit (Vector Laboratories) for 30 min. After further washing with PBST, a substrate solution consisting of $0.2\,mg\,mL^{-1}$ of 2,2′-Azino-bis(3-ethylbenzothiazoline-6-sulfonic acid) (ABTS) and 0.02% H_2O_2 in 0.1 M citrate buffer was added until a blue color developed and the OD was measured at 405 nm using a spectrophotometer. Plate-to-plate variations in OD readings were controlled using a common standard serum with an OD value of 0.350. For detecting anti-PGL-I antibody, NTP-BSA was coated at a concentration of $0.5\,\mu g\,mL^{-1}$, and the same procedure used to detect anti-MMP-II antibody was followed, except that the secondary antibody used was biotinylated anti-human IgM at a concentration of $1\,\mu g\,mL^{-1}$. The volume of all solutions used in the 96-well plate was $100\,\mu L\,well^{-1}$.

Statistical analyses

The data were analyzed using MEDCALC software (MedCalc, Belgium). A receiver operator characteristics (ROC) curve was drawn to calculate the cut-off levels. The McNemar test was applied (MMP-II vs. PGL-I test) to determine the P value. The P value of < 0.05 was considered to be statistically significant. The κ value was calculated to determine the agreement between the two tests.

Results and discussion

MMP-II (bfrA) has been previously identified as one of the components of *M. leprae* capable of stimulating $CD4^+$ and $CD8^+$ T cells (Maeda *et al.*, 2005). In multi-bacillary leprosy, *M. leprae* is widely disseminated and abundant antibody production is observed due to polyclonal B cell activation, while in pauci-bacillary leprosy, the bacilli are usually localized in skin lesions and type 1 T cells are predominantly activated, and so the level of antibodies to *M. leprae* antigens is usually low. However, preliminary experiments showed that the pooled pauci-bacillary leprosy sera reacted to MMP-II on polyvinylidene difluoride (PVDF) membranes.